

SYNTHESIS AND CHARACTERIZATION OF NEW CONDUCTING POLYMER- NANO  
PARTICLE COMPOSITES

A THESIS SUBMITTED TO  
THE GRADUATE SCHOOL OF NATURAL AND APPLIED SCIENCES  
OF  
MIDDLE EAST TECHNICAL UNIVERSITY

BY

ESRA EROĞLU

IN PARTIAL FULFILLMENT OF THE REQUIREMENTS  
FOR  
THE DEGREE OF MASTER OF SCIENCE  
IN  
CHEMISTRY

JANUARY 2013



Approval of the thesis:

**SYNTHESIS AND CHARACTERIZATION OF NEW CONDUCTING POLYMER-  
NANO PARTICLE COMPOSITES**

Submitted by **ESRA EROĞLU** in partial fulfillment of the requirements for the degree of **Master of Science in Chemistry Department, Middle East Technical University** by,

Prof. Dr. Canan Özgen  
Dean, Graduate School of **Natural and Applied Sciences**

\_\_\_\_\_

Prof. Dr. İlker Özkan  
Head of Department, **Chemistry**

\_\_\_\_\_

Prof. Dr. Ahmet M. Önal  
Supervisor, **Chemistry Dept., METU**

\_\_\_\_\_

Assist. Prof. Dr. Emren Nalbant Esentürk  
Co-Supervisor, **Chemistry Dept., METU**

\_\_\_\_\_

**Examining Committee Members:**

Assoc. Prof. Dr. Ali Çırpan  
Chemistry Dept., METU

\_\_\_\_\_

Prof. Dr. Ahmet Muhtar Önal  
Chemistry Dept., METU

\_\_\_\_\_

Assist. Prof. Dr. Emren Nalbant Esentürk  
Chemistry Dept., METU

\_\_\_\_\_

Assist. Prof. Dr. Seha Tirkeş  
Chemical Engineering and Applied Chemistry Dept.,  
ATILIM UNIVERSITY

\_\_\_\_\_

Assist. Prof. Dr. İrem Erel  
Chemistry Dept., METU

\_\_\_\_\_

Date: January 28, 2013

**I hereby declare that all information in this document has been obtained and presented in accordance with academic rules and ethical conduct. I also declare that, as required by these rules and conduct, I have fully cited and referenced all materials and results that are not original to this work.**

Name, Last name: Esra, Erođlu

Signature:

## ABSTRACT

### SYNTHESIS AND CHARACTERIZATION OF NEW CONDUCTING POLYMER- NANO PARTICLE COMPOSITES

Eroğlu, Esra

M.Sc., Department of Chemistry

Supervisor: Prof. Dr. Ahmet M. Önal

Co-Supervisor: Assist. Prof. Dr. Emren Nalbant Esentürk

January 2013, 38 Pages

In this study, conjugated monomers containing fluorene units; 2-(9,9-dihexyl-2-(thiophen-2-yl)-9H-fluoren-7-yl)thiophene (**TFT**) and 5-(9,9-dihexyl-2-(2,3-dihydrothieno[3,4-b][1,4]dioxin-5-yl)-9H-fluoren-7-yl)-2,3dihydrothieno[3,4b][1,4] dioxine (**EFE**) were synthesized on the basis of donor-acceptor-donor approach and their electrochemical polymerization were achieved via potential cycling. Optical and electrochemical properties of their corresponding polymers, poly(2-(9,9-dihexyl-2-(thiophen-2-yl)-9H-fluoren-7-yl)thiophene) **PTFT**, and poly(5-(9,9-dihexyl-2-(2,3-dihydrothieno[3,4-b][1,4]dioxin-5-yl)-9H-fluoren-7-yl)-2,3dihydrothieno[3,4b][1,4] dioxine) **PEFE**, were investigated and it was found that polymer films exhibited quasi-reversible redox behavior ( $E_{\text{pox}} = 1.10$  V for **PTFT**,  $E_{\text{pox}} = 0.70$  V and 1.00 V for **PEFE**) accompanied with a reversible electrochromic behavior, yellow to dark green for **PTFT**, yellow to parliament blue for **PEFE**. Their band gap values ( $E_g$ ) were found to be 2.36 eV and 2.26 eV for **PTFT** and **PEFE**, respectively. Furthermore, gold nanoparticles (AuNP) were prepared and their interaction with polymer films, **PTFT** and **PEFE**, were investigated using spectroscopic techniques. The fluorescence properties of the polymers and their composites, prepared by the interaction of AuNP with polymers, were also investigated.

**Keywords:** Conjugated polymers, fluorene, gold nanoparticles, polymer-gold nanoparticle composites.

## ÖZ

### YENİ İLETKEN POLİMER- NANOPARÇACIK KOMPOZİTLERİN SENTEZLENMESİ VE KARAKTERİZASYONU

Eroğlu, Esra  
Y. Lisans, Kimya Bölümü  
Tez Yöneticisi: Prof. Dr. Ahmet M. Önal  
Ortak Tez Yöneticisi: Yard. Doç.Dr. Emren Nalbant Esentürk

Ocak 2013, 38 sayfa

Bu çalışmada, verici-alıcı-verici dizininde, floren içeren konjuge monomerler 2-(9,9-dihexzil-2-(tiyofen-2-yl)-9H-floren-7-yl)tiyofen (**TFT**) ve 5-(9,9-dihexzil-2-(2,3-dihidrotyeno[3,4-b][1,4]dioksin-5-yl)-9H-floren-7-yl)-2,3dihidrotyeno[3,4b][1,4] dioksin (**EFE**) sentezlenmiş ve monomerler döngülü voltametri yöntemi ile elektrokimyasal olarak polimerleştirilmiştir. Elde edilen polimerlerin, poli(2-(9,9-dihexzil-2-(tiyofen-2-yl)-9H-floren-7-yl)tiyofen) (**PTFT**) ve poli(5-(9,9-dihexzil-2-(2,3-dihidrotyeno[3,4-b][1,4]dioksin-5-yl)-9H-floren-7-yl)-2,3dihidrotyeno[3,4b][1,4] dioksin) (**PEFE**), optik ve elektrokimyasal özellikleri incelenmiş ve polimer filmlerinin tersinir redoks davranımı esasına (**PTFT** için  $E_{\text{pox}} = 1.10$  V, **PEFE** için  $E_{\text{pox}} = 0.70$  V ve  $1.00$  V) tersinir elektrokromik davranım (**PTFT** için sarıdan koyu yeşile ve **PEFE** için sarıdan maviye) gösterdiği gözlenmiştir. **PTFT** ve **PEFE**' nin bant aralıkları sırasıyla 2.36 eV ve 2.26 eV olarak bulunmuştur. Ayrıca, altın nanotanecikler (AuNP) hazırlanmış ve polimer filmleri, **PTFT** ve **PEFE**, ile etkileşimleri spektroskopik teknikler kullanılarak incelenmiştir. Polimerlerin ve bunların AuNP ile etkileşimi sonucu elde edilen kompozitlerin floresan özellikleri de incelenmiştir.

**Anahtar Sözcükler:** Konjuge Polimerler, Floren, Altın nanoparçacık, Polimer- altın nanoparçacık kompozitleri.

TO MY PARENTS

## ACKNOWLEDGEMENTS

I would like to express my deepest gratitude to my supervisor Prof. Dr. Ahmet M. ÖNAL starting from the first day, he always encouraged me with his positive attitude. I sincerely appreciate the time and efforts he has taken to train me and improve my thesis.

I am grateful to Assist.Prof.Dr. Emren NALBANT ESENTÜRK for supporting and criticizing in every stage of this work.

I am thankful to Assoc. Prof. Dr. Atilla Cihaner for sharing his experience during my laboratory works.

I am also thankful to, Buket BEZGİN ÇARBAŞ, Merve İÇLİ ÖZKUT and labmates 'Prof. Dr. Ahmet M. Önal Research Group' for their help during my study.

I sincerely acknowledge my friends; Barış KARABAY, Özden ÇELİKBİLEK, Şeyma EKİZ, Elif ERTEM, Murat Kadir DELİÖMEROĞLU and Çağatay DENGİZ with whom I had spent matchless enjoyable time during my undergraduate and graduate years; without their encouragement I could not finish my master program.

I would like to extend my gratitude to my family for their endless love and support in every step of my life. I could not achieve any of these without their support.

## TABLE OF CONTENTS

<b>ABSTRACT</b> .....	<b>v</b>
<b>ÖZ</b> .....	<b>vi</b>
<b>ACKNOWLEDGEMENTS</b> .....	<b>viii</b>
<b>TABLE OF CONTENTS</b> .....	<b>ix</b>
<b>LIST OF FIGURES</b> .....	<b>xi</b>
<b>LIST OF TABLES</b> .....	<b>xii</b>
<b>LIST OF ABBREVIATIONS</b> .....	<b>xiii</b>
<b>CHAPTERS</b> .....	<b>1</b>
<b>1. INTRODUCTION</b> .....	<b>1</b>
1.1. Conducting Polymers (CPs) .....	1
1.1.1. Brief History of CPs .....	1
1.1.2. Conductivity of CPs .....	2
1.1.3. Band Theory .....	2
1.1.4. Electrochemical Polymerization.....	3
1.2. Polyfluorenes .....	4
1.2.1. Overview of Polyfluorenes .....	4
1.2.2. Synthesis of PFs .....	6
1.2.3. Fuctionalization of PFs .....	6
1.3. Brief Information of Nanoparticles (NPs).....	7
1.4. Surface Plasmon Oscillation (SPO).....	7
1.5. Properties of AuNPs .....	8
1.6. Preparation of AuNPs .....	9
1.7. Composite Materials .....	9
1.8. Aim of Study.....	10
<b>2. EXPERIMENTAL</b> .....	<b>11</b>
2.1. General Information.....	11
2.2 Monomer Synthesis .....	11
2.2.1 Synthesis of 2-(9,9-dihexyl-2-(thiophen-2-yl)-9H-fluoren-7-yl)thiophene (TFT) .....	11
2.2.2 Synthesis of 5-(9,9-dihexyl-2-(2,3-dihydrothieno[3,4-b][1,4]dioxin-5-yl)-9H-fluoren-7-yl)-2,3dihydrothieno[3,4b][1,4] dioxine (EFE) .....	12
2.3 Polymer Synthesis .....	12
2.3.1. Electrochemical polymerization of monomers .....	12
2.4. AuNP preparation.....	13
2.5. Polymer-Gold Nanoparticle Composite Preparation .....	13
2.6. Characterization of Polymer .....	13
2.6.1. Cyclic Voltammetry (CV) .....	13

2.7. Spectroelectrochemistry .....	13
2.8. Kinetic Properties .....	13
2.9. Characterization of Polymer-Gold nanoparticle composites .....	13
2.9.1. UV Measurements .....	14
2.9.2. Scanning Electron Microscope (SEM).....	14
<b>3. RESULTS AND DISCUSSION .....</b>	<b>15</b>
3.1. Electrochemical Properties of Monomers .....	15
3.1.1. Cyclic Voltammograms of Monomers .....	15
3.1.2. Electropolymerization of Monomers .....	16
3.2. Characterization of Polymers .....	17
3.2.1. Electrochemical Properties of Polymers .....	17
3.3. Properties of Composite Materials .....	19
3.3.1. UV-Vis Measurements.....	19
3.3.2. Scanning Electron Microscope (SEM) Images .....	19
3.4. Comparison of Polymer-Au NP composites .....	23
3.4.1. Comparison of Spectroelectrochemical Properties of Polymers and Composites .....	23
3.4.2. Comparison of Kinetic Properties of Polymers and Composites .....	26
3.4.3. Comparison of Fluorescence Properties of Polymers and Composites .....	27
<b>4. CONCLUSION .....</b>	<b>31</b>
<b>REFERENCES.....</b>	<b>33</b>
<b>APPENDICES .....</b>	<b>36</b>
<b>A. NUCLEAR MAGNETIC RESONANCE SPECTRA OF TFT AND EFE MONOMERS .....</b>	<b>36</b>
<b>B. FTIR SPECTRA OF MONOMERS AND POLYMERS.....</b>	<b>38</b>

## LIST OF FIGURES

### FIGURES

<b>Figure 1:</b> Examples of some CPs and their repeating unit .....	1
<b>Figure 2:</b> Formations of charge carriers and polaron/bipolaron structures in polypyrrole during oxidative doping <sup>19</sup> .....	2
<b>Figure 3:</b> Schematic representation of three types of materials in terms of their band gaps <sup>22</sup> .....	3
<b>Figure 4:</b> Mechanism of electrochemical polymerization of heterocyclic monomers (X = O, S, and NH) .....	4
<b>Figure 5:</b> Different copolymers of PFs .....	5
<b>Figure 6:</b> PFs covering whole visible spectrum .....	5
<b>Figure 7:</b> Polyfluorene with typical ring numbering .....	7
<b>Figure 8:</b> Band gap values of different kinds of fluorene copolymers .....	7
<b>Figure 9:</b> Schematic presentation of the surface plasmon in metallic NPs when metal sphere interacts with electromagnetic radiation .....	8
<b>Figure 10:</b> Absorption spectra of AuNPs with different diameters in organic solvent at room temperature. <sup>70</sup> .....	9
<b>Figure 11:</b> Synthesis of 2-(9,9-dihexyl-2-(thiophen-2-yl)-9H-fluoren-7-yl)thiophene (TFT) .....	12
<b>Figure 12:</b> Synthesis of 5-(9,9-dihexyl-2-(2,3-dihydrothieno[3,4-b][1,4]dioxin-5-yl)-9H-fluoren-7-yl)-2,3-dihydrothieno[3,4b][1,4] dioxine (EFE) .....	12
<b>Figure 13:</b> Cyclic voltammograms of a) TFT in 0.1 M TBABF <sub>4</sub> /DCM/ACN b) EFE in 0.1 M TBAPF <sub>6</sub> /DCM/BF <sub>3</sub> O(C <sub>2</sub> H <sub>5</sub> ) <sub>2</sub> solution at 100 mV/s vs. Ag/AgCl. Concentration of monomers: TFT= 5.0 x10 <sup>-3</sup> M, EFE= 4.0 x10 <sup>-3</sup> .....	15
<b>Figure 14:</b> Electropolymerization of a) 5.0 x 10 <sup>-3</sup> M of TFT in ACN/ DCM (98/2; v/v) with 0.1M TBABF <sub>4</sub> , b) 4.0 x 10 <sup>-3</sup> M of EFE in DCM/ BF <sub>3</sub> O(C <sub>2</sub> H <sub>5</sub> ) <sub>2</sub> with 0.1 M TBAPF <sub>6</sub> at 100 mV/s (vs. Ag/AgCl) .....	16
<b>Figure 15:</b> Cyclic voltammograms of films a) PTFT in 0.1 M TBABF <sub>4</sub> /ACN b) PEFE in 0.1M TBAPF <sub>6</sub> / ACN on a Pt disk electrode at 100 mV/s (vs. Ag/AgCl). .....	17
<b>Figure 16:</b> (a) Scan rate dependence of PTFT and PEFE film on a Pt disk electrode in 0.1 M TBABF <sub>4</sub> /ACN and TBAPF <sub>6</sub> /ACN between 20-100 mV/s. (b) Relationship of anodic (ip,a) and cathodic (ip,c) current peaks as a function of scan rate between neutral and oxidized state .....	18
<b>Figure 17:</b> UV-vis absorption spectra of a) PTFT-AuNPs b) PEFE- AuNPs composites in ACN .....	19
<b>Figure 18:</b> SEM images of PTFT and PTFT-AuNP composites with respect to polymer –Au interaction times a) PTFT b) 1h c) 2h d) 3h e) 4h in AuNP solution .....	21
<b>Figure 19:</b> SEM images of PEFE and PEFE-AuNP composites with respect to polymer –Au interaction times a) PTFT b) 1h c) 2h d) 3h e) 4h in AuNP solution .....	22
<b>Figure 20:</b> Optical absorption spectra of a) PTFT c) PEFE on ITO b) Optical absorption spectra of PTFT-AuNP d) PEFE-AuNP composites on ITO electrode electrode in 0.1 M TBABF <sub>4</sub> /ACN and TBAPF <sub>6</sub> /ACN respectively at potential range between 0.0V and 1.20V. ....	25
<b>Figure 21:</b> Fluorescence spectra of a) PTFT and PTFT/ AuNP composite b) PEFE and PEFE/ AuNP composite solution in toluene at room temperature .....	28

## LIST OF TABLES

### TABLES

<b>Table 1:</b> Colors of the <b>PTFT</b> , <b>PEFE</b> on ITO electrodes in their neutral and oxidized state.....	26
<b>Table 2:</b> Optical and electrochemical properties of <b>PTFT</b> , <b>PEFE</b> , <b>PTFT/AuNP</b> and <b>PEFE/ AuNP</b> composites.....	27
<b>Table 3:</b> Fluorescence emissions of <b>PTFT</b> , <b>PEFE</b> , <b>PTFT/AuNP</b> , <b>PEFE/ AuNP</b> composites in toluene.....	29

## LIST OF ABBREVIATIONS

<b>ACN</b>	Acetonitrile
<b>AuNP</b>	Gold nanoparticle
<b>SPO</b>	Surface Plasmon Oscillation
<b>CB</b>	Conduction Band
<b>CP</b>	Conjugated Polymer
<b>CE</b>	Coloration Efficiency
<b>CV</b>	Cyclic Voltammetry
<b>DAD</b>	Donor Acceptor Donor
<b>DCM</b>	Dichloromethane
<b>EFE</b>	Poly5-(9,9-dihexyl-2-(2,3-dihydrothieno[3,4-b][1,4]dioxin-5-yl)-9H-fluoren-7-yl)- 2,3dihydrothieno[3,4b ][1,4] dioxine
<b>HOMO</b>	Highest Occupied Molecular Orbital
<b>ITO</b>	Indium-tin oxide
<b>LUMO</b>	Lowest Unoccupied Molecular Orbital
<b>NMR</b>	Nuclear Magnetic Resonance
<b>TFT</b>	(2-(9,9-dihexyl-2-(thiophen-2-yl)-9H-fluoren-7-yl)thiophene)
<b>PTFT</b>	Poly (2-(9,9-dihexyl-2-(thiophen-2-yl)-9H-fluoren-7-yl)thiophene)
<b>PEFE</b>	Poly5-(9,9-dihexyl-2-(2,3-dihydrothieno[3,4-b][1,4]dioxin-5-yl)-9H-fluoren-7-yl)- 2,3dihydrothieno[3,4b ][1,4] dioxine
<b>Pt</b>	Platinum
<b>PF</b>	Polyfluorene
<b>RE</b>	Reference Electrode
<b>SPEL</b>	Spectroelectrochemical
<b>TBABF<sub>4</sub></b>	Tetrabutylammoniumtetrafluoroborate
<b>TBAPF<sub>6</sub></b>	Tetrabutylammoniumhexafluorophosphate
<b>VB</b>	Valence Band
<b>UV-VIS</b>	Ultraviolet Visible
<b>WE</b>	Working Electrode
<b>Δ%T</b>	Percent Transmittance



## CHAPTER 1

### INTRODUCTION

#### 1.1. Conducting Polymers (CPs)

##### 1.1.1. Brief History of CPs

Conducting polymers (CPs) are macro molecules which are formed by polymerization of conjugated chains in which  $\pi$ -electrons are delocalized along the chain. The important developments in the field of CPs have started with the coincidental discovery in a collaborative effort between three scientist, H. Shirakawa, A. J. Heeger and A. McDiarmid, that polyacetylene exposed to iodine vapors develops very high and well characterized conductivities for an organic material.<sup>1</sup> In 2000, Nobel Prize was given to H. Shirakawa, A. J. Heeger and A. McDiarmid, who invented high conductivity property of polyacetylene upon iodine doping, in chemistry.<sup>2-3</sup> Although polyacetylene was initially the most studied CP from scientific and practical application point of view, due to its high chemical instability in air, limited processibility and low solubility, interest in it has recently been confined to its scientific aspects.<sup>4</sup> Thus, considerable research done on polyacetylene to overcome its limiting properties which is accompanied with the rapid development of many other CPs in the following years. Polypyrrole<sup>5</sup>, polyfuran<sup>6</sup>, polythiophene<sup>7,8</sup> and poly(3,4-ethylenedioxythiophene) (PEDOT)<sup>9</sup>, which are similar properties with some other aromatic polymers like polyaniline<sup>10</sup>, poly(p-phenylenevinylene)<sup>11</sup> and polyfluorenes<sup>12</sup> are some examples of other conjugated polymers which are shown in Figure 1. These polymers have attracted considerable attention since they found wide variety of applications including light-emitting diodes<sup>13</sup>, molecular electronics<sup>14</sup>, organic solar cells<sup>15</sup>, gas sensors<sup>16</sup> and electrochromic mirrors.<sup>17</sup> These potential applications make CPs center of attention and significant efforts have been devoted for the design and synthesis of new  $\pi$ -conjugated polymers.

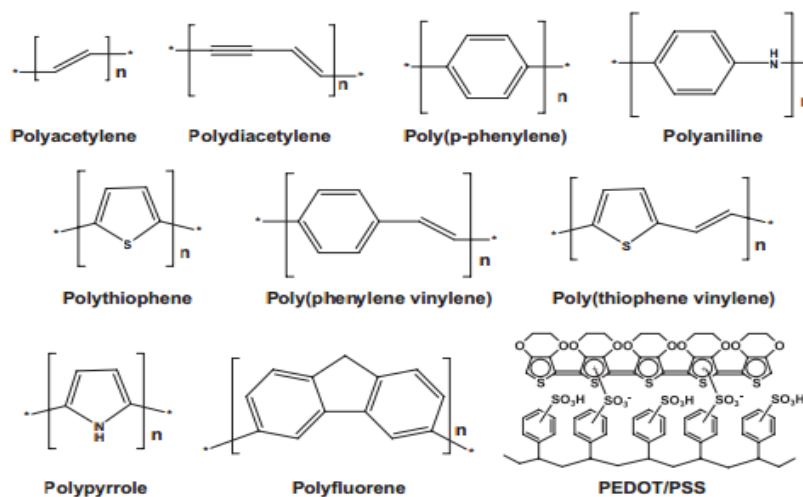


**Figure 1:** Examples of some CPs and their repeating unit

### 1.1.2. Conductivity of CPs

Conjugated polymers exhibit a variety of interesting properties among them their ability to act as electronic conductors is perhaps the most important. Electronically conducting polymers are extensively conjugated molecules, with alternating single and double bonds along the chains. This characteristic structural feature of conjugated polymers makes them semi-conductors in their neutral state.

To conduct electricity, charge carriers should be introduced into the polymer along  $\pi$  orbitals by a process known as doping. In this manner, positive (p-type) and negative (n-type) charge carriers could be formed during polymer oxidation and reduction, respectively. Formation of either p or n type charge carriers with the distortion of structure is named as polaron. If two polarons form a couple, it turns into bipolaron with a charge of +2 or (-2) shown in Figure 2. As the number of bipolarons increases, the number of states between the valence band and conduction band also increases. As a result, band gap,  $E_g$ , of polymer decreases and conductivity increases at the same time.<sup>18</sup>

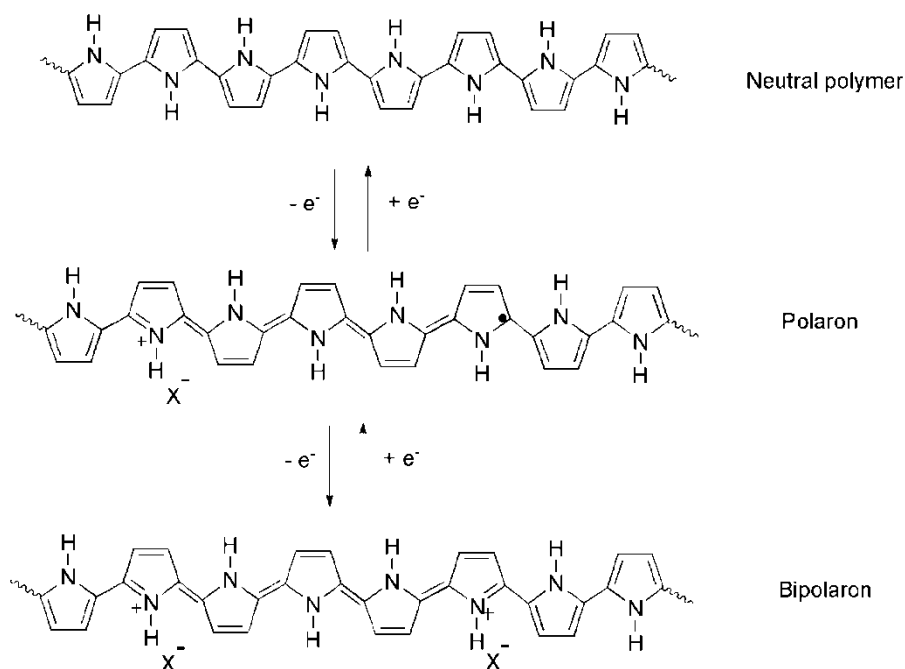


**Figure 2:** Formations of charge carriers and polaron/bipolaron structures in polypyrrole during oxidative doping<sup>19</sup>

### 1.1.3. Band Theory

Materials could be classified into three main categories according to their conducting properties as insulators, semiconductors and conductors. To predict the fundamental category of material, major reference have to be known is the band gap. A band gap ( $E_g$ ) is defined as energy difference between highest occupied molecular orbital (HOMO) and lowest unoccupied molecular orbital (LUMO).<sup>20</sup> An insulator has such a high band gap energy that is insufficient to allow electrons to promote from valence band to the conduction band.  $E_g$  value of insulator is generally greater than 3.0 eV. Thus, valence band is fully occupied and conduction band is fully empty.

A band gap energy of semiconductor, on the other hand, is lower compared to insulator, which is between 0.5 - 3.0 eV, so that electrons could be excited from the valence band to the conduction band with different kinds of excitations. If overlapping of valence and conduction bands occurs the  $E_g$  value becomes zero and the material gains high electrical conduction property<sup>21</sup> as in the case of conductors. (Figure 3)

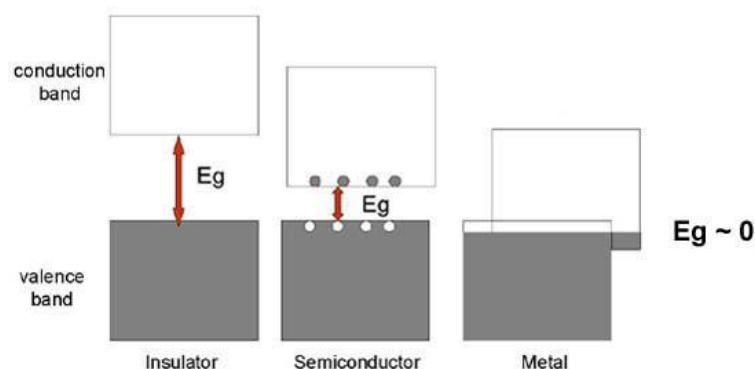


**Figure 3:** Schematic representation of three types of materials in terms of their band gaps<sup>22</sup>

#### 1.1.4. Electrochemical Polymerization

In general CPs can be synthesized either by chemical polymerization or by electrochemical polymerization methods.<sup>23-26</sup> Electrochemical polymerization is one of the polymerization technique in which polymerization is initiated via formation of radical ions due to the oxidation of monomer by an applied external potential. Electrochemical polymerization has been widely used to generate CPs due to its many advantages as stated below.<sup>27-28</sup>

- Properties of product could be analyzed in situ.
- Small amount of monomer is sufficient to start polymerization.
- Product obtained from electrochemical polymerization could adhere well to the electrode surface.
- Product shows good electrochromic properties.
- The redox system could be altered by providing control of doping-dedoping process, adjusting applied voltage, polymerization time or scan rate.

There are some important points that affect the electrochemical polymerization process and properties of the resultant polymer such as solvent-electrolyte couple, applied voltage and monomer concentration<sup>29</sup>. First of all, solvent should be able to dissolve both monomer and supporting electrolyte. However, if there is a need for polymer film on the electrode surface, polymer should be insoluble in the solvent. Electrolyte has to be non-nucleophilic and inert through electrochemical reactions. Tetraalkylammonium hexafluorophosphate, tetraalkylammonium tetrafluoroborate and lithium perchlorate are mostly preferred electrolytes in the synthesis of CPs<sup>30</sup>. Also, oxidation/reduction potentials of the solvent-electrolyte couple should be greater than the redox potential of the monomer. Monomer concentration is also critical for successful electrochemical polymerization and it should be high enough to ensure polymer synthesis. Finally, applied potential should not exceed the oxidation potential of monomer to prevent the overoxidation and side reactions.<sup>31</sup>

The first step of electrochemical polymerization is the formation of radical cation by the oxidation of monomer via applied potential.

Due to higher speed of electron transfer reactions compared to monomer diffusion, radical cations maintain high concentrations near the electrode surface during the polymerization.

In the second step, two radical cations are coupled and make re-aromatization by losing two hydrogen atoms. Then, dimer is oxidized and turns into radical form to couple with monomeric radical. Polymerization proceeds until oligomer becomes insoluble and starts to adhere to the electrode surface. Figure 4 represents the mechanism of electro-oxidative polymerization of heterocyclic monomers.<sup>32</sup>

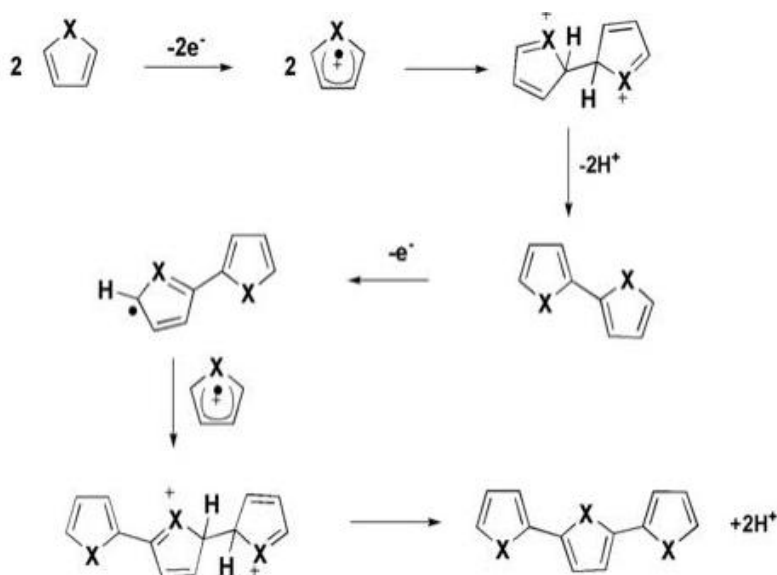


**Figure 4:** Mechanism of electrochemical polymerization of heterocyclic monomers (X = O, S, and NH)<sup>33</sup>

## 1.2. Polyfluorenes

### 1.2.1. Overview of Polyfluorenes

Among the variety of conjugated polymers, polyfluorenes, PFs, are suitable for wide range of applications due to their high photoluminescence quantum yields, good photostability and high thermal stability. They are also one of the most preferred candidates of blue electroluminescence devices.<sup>34-35</sup> On the other hand, it has too high energy barrier to inject a hole and limited solubility property which are some of the disadvantages of PF. Furthermore, PFs may show excimer and aggregate formation when exposed to high temperatures or during current flow. In both cases, red-shift in the fluorescence with reduced intensity occurs.<sup>36</sup> To prevent these drawbacks, C-9 position of the fluorene might be substituted by suitable substituents which may not only increase the solubility but also avoids aggregate formation. Another possibility is copolymerizing fluorene with other suitable monomers which will allow the tuning of emission colors. Furthermore, stiffness and liquid crystalline characteristics of PFs might also be affected depending on the nature of comonomer used in the copolymerization. Some possible comonomers are depicted in Figure 5.<sup>37</sup> Examples of copolymers of PFs with different emission colors are depicted in Figure 6.

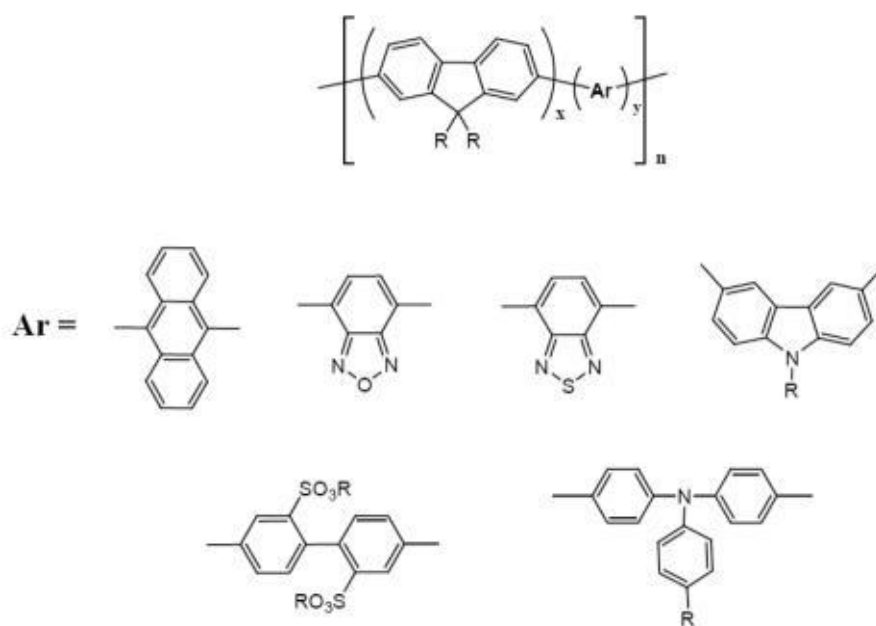


**Figure 5:** Different copolymers of PFs

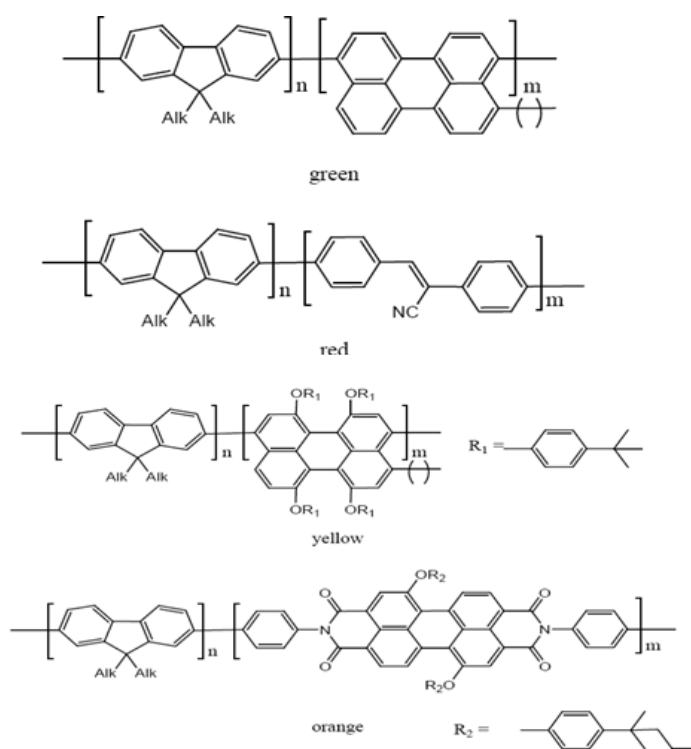


**Figure 6:** PFs covering whole visible spectrum

### 1.2.2. Synthesis of PFs

There are two common methods for the synthesis of PFs by carbon-carbon cross coupling reactions from fluorene monomers. First method was reported by Yoshino and coworkers in which poly (9, 9-dihexyl-2, 7-fluorene) is synthesized via oxidative coupling reaction by using iron (III) chloride as catalyst.<sup>38-39</sup> This method was named as Scholl reaction. However, there are some drawbacks of this reaction including formation of low molecular weight product and nonconjugated linkages other than 2 and 7 positions. Thus, new method, transition-metal mediated polycondensation reactions, has been replaced by Schroll reaction in many syntheses.

Transition-metal mediated polycondensation reactions branched into three according to the types of transition metals used. Yamamoto, Suzuki and Stille coupling reactions are the methods in which nickel used for Yamamoto, palladium for Suzuki and Stille coupling as catalysts. Products obtained by Yamamoto coupling are limited if the object is to synthesize homopolymer and copolymer. On the other hand, high molecular weight polymer and wide range of PF homo and copolymer synthesis are possible when Suzuki and Stille coupling methods are used.<sup>40</sup>

### 1.2.3. Fuctionalization of PFs

PFs are important class of conjugated polymers due to their light emitting properties with high photoluminescence quantum yields. Furthermore, they exhibit high chemical and thermal stabilities which allow them to be used in light emitting diodes. However, PFs also have some disadvantages such as formation of excimers and bias to aggregation in the solid state, and lower solubility in common solvents.<sup>41-43</sup>

One way to overcome these drawbacks is the substitution of the C-9 position of fluorene by suitable substituents, such as aryl or alkyl groups. If alkyl groups are attached to the C-9 position of fluorene, solubility is improved in common organic solvents so that processibility will increase. Some aryl groups such as carbazole and oxadiazole could be attached to the C-9 position of fluorene unit. All these side groups have some effect on the morphology of PFs and PFs with different morphology show different photophysical properties.<sup>44</sup>

Besides functionalization of the C-9 position of fluorene, copolymerization of fluorene with different kind of aryl partners makes possible altering of electronic properties so that this method becomes important for PFs whose electronic properties are not easily altered by chemical modifications.<sup>45</sup>

Copolymerization typically starts and continues from the 2-7 or 3-6 positions of fluorene unit. This process could be performed by Stille coupling reaction in which fluorene monomer should be brominated and comonomer should be stannated before the coupling reaction. As a result of copolymerization, band gaps of polymers are changed and different colored materials could be obtained. It is revealed that alternation of donor and acceptor groups regularly could reduce the band gap by means of broadening of the valence and conduction bands.<sup>46</sup> Therefore, various donor-acceptor type copolymers based on fluorene were prepared. Some examples of fluorene containing copolymers synthesized in our research groups are shown in Figure 8.<sup>47-50</sup>

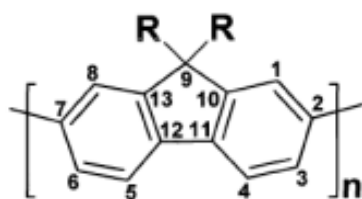


**Figure 7:** Polyfluorene with typical ring numbering

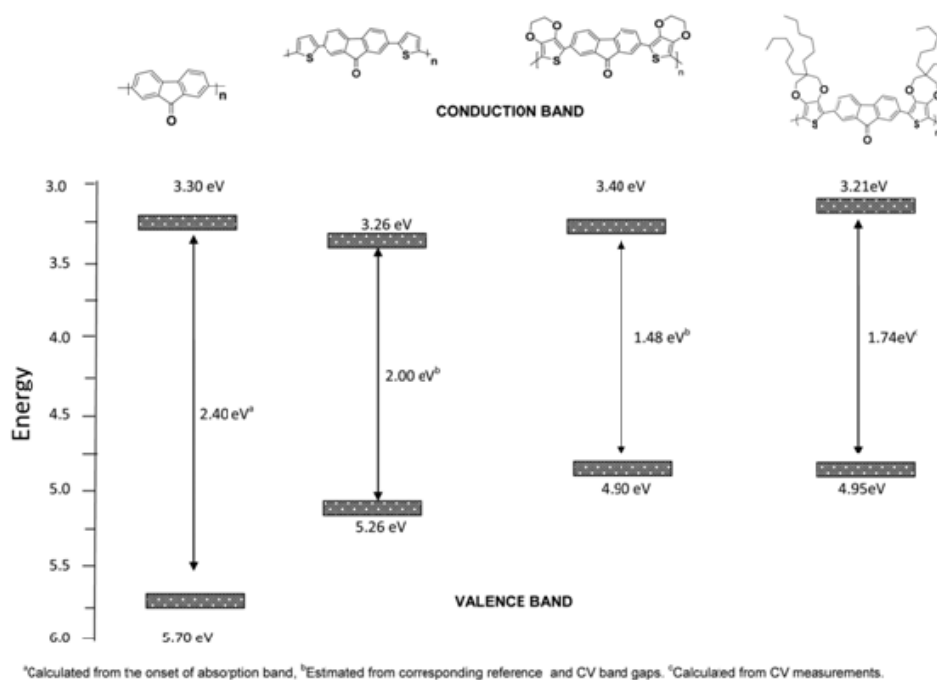


**Figure 8:** Band gap values of different kinds of fluorene copolymers

### 1.3. Brief Information of Nanoparticles (NPs)

Particles which have the dimensions in the scale of 1-100 nm are called nanoparticles (NPs), whether they are dispersed in gaseous, liquid, or solid media. NPs usually contain  $10^6$  atoms or fewer and they bond together and are intermediate in size between individual atoms and macroscopic solids.<sup>51-52</sup> NPs have attracted the interest of many scientist in different fields of chemistry, physics and material science due to their unique physical and chemical properties.<sup>53-57</sup> Specifically, studies with gold nanoparticles (AuNPs) have become an active area in recent years because they can be used succesfully in electronical, optical and catalytic studies.<sup>58-59</sup>

### 1.4. Surface Plasmon Oscillation (SPO)

The electric field of an incoming light causes polarization of the free conduction electrons of spherical nanoparticles. The positive charges are assumed to be immobile and the negative charges that is, the conduction electrons, start to move by applied electric field. Thus, such kind of displacement of

conduction electrons from the positive charges results to net charge difference at the boundaries of NPs. As a consequence, there is a dipolar oscillation of the electrons with a specific time period, which is named as surface plasmon oscillation. In other words, the conduction electrons in a spherical cluster are in resonance with the frequency of incoming light and results to surface plasmon oscillations (SPO). SPO is generally referred as surface plasmon resonance. This resonance frequency is strongly dependent on the size, shape, interparticle interactions, and local environment of the nanoparticle.<sup>60-65</sup> Figure 9 represents the creation of surface plasmon oscillation in metal NPs.

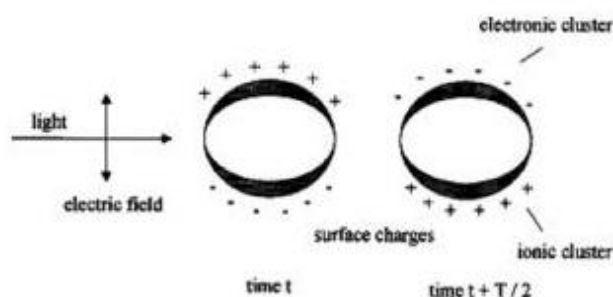


**Figure 9:** Schematic presentation of the surface plasmon in metallic NPs when metal sphere interacts with electromagnetic radiation

### 1.5. Properties of AuNPs

Spherical AuNPs are preferred for many purposes in different areas due to their shape and size related optoelectronic properties, low toxicity, large surface-to volume ratios and biocompatibility.

One of the most important properties of AuNPs is their surface plasmon resonance ability which results with absorption of light in visible region. Due to the fact that d-d band transitions matches with the energy of light in the visible region, AuNPs characteristically show strong absorption in the visible region.<sup>66</sup> They show a range of colors such as orange, purple, red or brown as the particle size, solvent, temperature changes.<sup>67-69</sup> For small gold nanoparticles with an average diameter about 30 nm generally have an absorption of light at about 520 and 530 nm. As the particle size gets bigger which is between 50-100 nm, in which amount of scattering light and peak broadening increase, absorption of light is observed between 540 and 570 nm. Figure 10 exhibits absorbances of AuNPs with respect to their increasing diameter sizes.

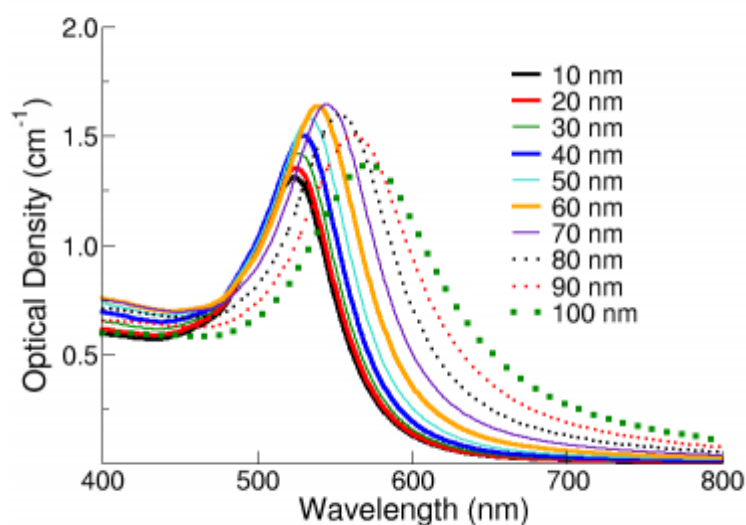


**Figure 10:** Absorption spectra of AuNPs with different diameters in organic solvent at room temperature.<sup>70</sup>

Second major point related with AuNPs is their fluorescence quenching property. This fluorescence deactivation process is based on good overlapping of excited fluorophores and the surface plasmon band of AuNPs. That is, if life time of emission is decreased; then, fluorophore's oscillating dipole is in phase with AuNPs surface plasmon resonance frequency.<sup>71</sup>

### 1.6. Preparation of AuNPs

Generally gold nanoparticles are produced in a liquid by reduction of chloroauric acid,  $H[AuCl_4]$ , with citric acid. This method is pioneered by J. Turkevich and named as Turkevich method. Although, the method is widely used for long times to synthesize AuNPs with diameter of 10-20 nm to 100 nm, it suffers from aggregation of NPs during thiolate processing. Therefore, to overcome aggregation problems new strategies were developed.<sup>72</sup>

In 1994, Brust and Schiffrin achieved to develop a new methodology having more advantages over former method. They followed biphasic reduction process in which tetraoctylammonium bromide (TOAB) was used as phase transfer catalyst and sodium borohydride ( $NaBH_4$ ) as the reducing agent. Final products, AuNPs, are soluble in organic phase and have high stability when compared to other AuNPs because of strong thiol-gold interactions and van der Waals attractions between the neighboring ligands. This high stability makes them possible to use for further functionalization.<sup>73</sup>

### 1.7. Composite Materials

The term 'composite' is used to identify two or more constituents that are gathered with different methods; then, product which have different physical and chemical behaviors than constituents. Also, nanocomposite materials have recently been studied due to their unique properties. Specifically, conducting polymers and metal nanoparticles have gained much attention in recent years because of their application areas such as catalysis<sup>74</sup>, optoelectronic devices<sup>75</sup>, transistors<sup>76</sup> and sensors<sup>77</sup>. Polyaniline, polythiophene and polypyrrole are the examples of conducting polymers and Au, Ag, Pt or Pd are the metal nanoparticles preferred to prepare nanocomposites.

Electrical and optical properties of these composite systems depend of the polymer and metal nanoparticle types and amounts. If AuNP and conducting polymer composites are considered, several methods have been studied by now in literature.<sup>78-81</sup>

Two of the most preferable methods are generally either adsorption of AuNPs on the substrate coated surfaces with bifunctional aminosiloxane and mercapto siloxane as terminal ligand or with n-alkanethiol containing terminal thiol and amine functional groups. The other popular method is embedding AuNPs into the polymer matrix by which effective stacking of AuNPs onto polymer surface and increase of stabilization of polymer are aimed. The final method stated in literature is the chemical and electrochemical polymerization in the presence of AuNPs.<sup>82-88</sup>

### **1.8. Aim of Study**

It is known that composite preparation has promising method to develop the conducting polymer properties in terms of electrical conductivity, fluorescence ability and optical properties. Thus, the main object of this study was to prepare AuNP containing conjugated polymers and to investigate the effect of AuNPs on the properties of polymer. For this purpose two types of monomers **TFT** and **EFE**, having D-A-D system to lower the band gap, have been designed and synthesized as a first step. Then, monomers were electropolymerized. After their characterization, AuNP containing composites were prepared to investigate the effect of AuNPs on the properties of electrochemically obtained polymers **PTFT** and **PEFE**. Optical and fluorescence properties of the polymers were compared with polymer film-AuNP composites.

## CHAPTER 2

### EXPERIMENTAL

#### 2.1. General Information

All chemicals were purchased from Sigma Aldrich and they were used without additional process except some solvents such as acetonitrile (ACN), toluene and dichloromethane (DCM). In the experiments, solvents were freshly distilled over CaH<sub>2</sub> under argon atmosphere before using. In electrochemical experiments, three-electrode setup was used containing platinum wire as counter electrode, platinum disc (0.02 cm<sup>2</sup>) as working electrode and Ag/AgCl in 3 M NaCl (aq) solution as a reference electrode. In these experiments, tetrabutylammonium hexafluorophosphate (TBAPF<sub>6</sub>) and tetrabutylammonium tetrafluoroborate (TBABF<sub>4</sub>) were used as electrolytes. Cycling voltammetry (CV) was used to synthesize and characterize polymers by potential cycling and constant potential electrolysis methods; then, behaviors of resulting films regarding electrochemically and optically and composite materials were analyzed in appropriate solvent-electrolyte mixture. Gamry PCI4/300 potentiostat-galvanostat was used for CV studies. During redox switching, all electronic transition changes that shows the spectroelectrochemical (SPEL) properties of CPs, were investigated on an indium tin oxide conducting glass (ITO, Delta Tech. 8–12 Ω, 0.7 cm x 5 cm) which was used as working electrode and with Ag wire as a pseudo-reference as reference and platinum wire as a counter electrode. A Hewlett-Packard 8453A diode array UV-vis spectrometer was used both for SPEL studies and to monitor AuNP formation on the polymer films. Also, FEI-Quanta 400 F scanning electron microscope (SEM) was used as complementary instrument to UV-Vis spectrometer to detect Au NPs. <sup>1</sup>H NMR and <sup>13</sup>C NMR spectra were recorded on a Bruker Spectrospin Avance DPX-400 Spectrometer in CDCl<sub>3</sub> using tetramethylsilane as the internal standard. FTIR spectra were recorded on a Bruker Vertex 70 spectrophotometer equipped with attenuated total reflectance (ATR) unit. High resolution mass spectrometry analysis was done via Water, Synapt HRMS instrument for characterization of monomers.

#### 2.2 Monomer Synthesis

##### 2.2.1 Synthesis of 2-(9,9-dihexyl-2-(thiophen-2-yl)-9H-fluoren-7-yl)thiophene (TFT)

2,7-dibromo-9,9-dihexyl-9H-fluorene (2.03 mmol, 1 equiv), 2-(Tributylstannyl)thiophene (4.06 mmol, 2 equiv) and 2 mol % of Pd(PPh<sub>3</sub>)<sub>4</sub> (0.082 mmol) were placed in a 100 ml two necked flask equipped with reflux condenser and magnetic stir bar under Ar atmosphere. 50 ml toluene, which had been freshly distilled and degassed with Ar, was added to the reaction medium as solvent and heated until the reflux starts which is about 100-110C°. It was stirred at stable reflux temperature and controlled with TLC. The reaction was stopped after 72 h and excess toluene was removed from the reaction medium under reduced pressure. The crude product was isolated by column chromatography on silica gel by eluting with chloroform: hexane (1:3, v/v). The purified pale yellow solid was isolated in a %65 yield. <sup>1</sup>H NMR (400 MHz, CDCl<sub>3</sub>): δ 7.76 (d, J= 8.2 Hz, 2H), 7.68-7.60 (m, 4H), 7.38 (d, J=4.4, 2H) 7.35-7.23 (m, 2H), 7.12 (d, 2H), 2.08 (q, J= 7.6, 2H, CH<sub>2</sub>), 1.46-1.12 (m, 26H, CH<sub>2</sub>), 1.24 (m, 4H, CH<sub>2</sub>), 0.92 (t, J=7.2, CH<sub>3</sub>). <sup>13</sup>C NMR (400 MHz, CDCl<sub>3</sub>) δ: 151.39, 142.36, 139.45, 137.97, 124.92, 120.39, 119.68, 118.43, 97.22, 55.18, 40.30, 31.46, 29.68, 23.72, 22.56, 14.02.

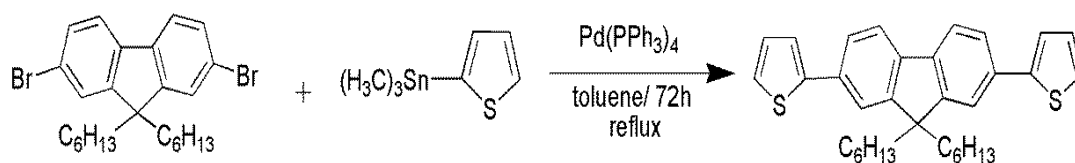


**Figure 11:** Synthesis of 2-(9,9-dihexyl-2-(thiophen-2-yl)-9H-fluoren-7-yl)thiophene (TFT)

### 2.2.2 Synthesis of 5-(9,9-dihexyl-2-(2,3-dihydrothieno[3,4-b][1,4]dioxin-5-yl)-9H-fluoren-7-yl)-2,3-dihydrothieno[3,4b][1,4] dioxine (EFE)

2,7-dibromo-9,9-dihexyl-9H-fluorene (1.42 mmol, 1 equiv), 2-(tributylstannyl)EDOT (2.8 mmol, 2 equiv) and 2 mol % of  $\text{Pd}(\text{PPh}_3)_2\text{Cl}_2$  (0.056 mmol) were placed in a 100 ml two necked flask equipped with reflux condenser and magnetic stir bar under Ar atmosphere. Freshly distilled and degassed 40 ml toluene was added to the reaction medium as solvent and heated until the reflux starts which is about 100-110°C. After stabilizing the temperature, reaction was stirred at reflux temperature and controlled with TLC until the end of the reaction. It was stopped after 72 h and toluene was removed by rotary evaporator. Monomer was isolated from the crude product by column chromatography on silica gel by chloroform: hexane (1:3.5, v/v) as an eluent. The resultant yellow solid was isolated in a %42 yield in yellow solid form.  $^1\text{H}$  NMR (400 MHz,  $\text{CDCl}_3$ ):  $\delta$  7.76 (d,  $J = 8.2$  Hz, 2H), 6.25 (s, 2H) 1.94 (t,  $J = 4.2$ , 4H,  $\text{CH}_2$ ), 1.52-0.96 (m, 16H,  $\text{CH}_2$ ), 0.72 (m, 4H,  $\text{CH}_2$ ), 0.67 (t,  $J = 7.2$ , 6H,  $\text{CH}_3$ ).  $^{13}\text{C}$  NMR (400 MHz,  $\text{CDCl}_3$ ):  $\delta$ : 151.39, 142.36, 139.45, 137.97, 124.92, 120.39, 119.68, 118.43, 97.22, 55.18, 40.30, 31.46, 29.68, 23.72, 22.56, 14.02.

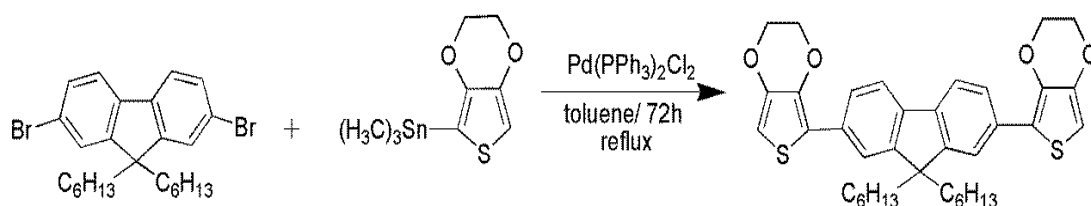


**Figure 12:** Synthesis of 5-(9,9-dihexyl-2-(2,3-dihydrothieno[3,4-b][1,4]dioxin-5-yl)-9H-fluoren-7-yl)-2,3-dihydrothieno[3,4b][1,4] dioxine (EFE)

## 2.3 Polymer Synthesis

### 2.3.1. Electrochemical polymerization of monomers

Electrochemical polymerization of both monomers, **TFT** and **EFE**, were performed by using multiple scan cyclic voltammetry. **TFT** ( $5.0 \times 10^{-3}$  M) was electropolymerized by using mixtures of ACN/ DCM (98/2 v/v) and  $\text{TBABF}_4$  as electrolyte on platinum disc electrode by repetitive potential cycling which was applied between 0.00 V and 1.27 V at a scan rate of 100 mV/s. Due to limited solubility of **TFT** in ACN it was first dissolved in limited amount of DCM. Polymerization of **EFE** was achieved on platinum electrode by repetitive potential cycling in between 0.00 V and 1.35 V at scan rate of 100 mV/s under Ar atmosphere. Polymerization was carried out in solvent mixture of DCM/ $\text{BF}_3\text{O}(\text{C}_2\text{H}_5)_2$  (99/1 v/v) and  $1 \times 10^{-3}$  M  $\text{TBAPF}_6$  was used as supporting electrolyte. After predetermined number of potential cycling, polymer film coated working electrodes were removed from the electrolytic solution and polymer films were washed with ACN to remove unreacted monomers and electrolytes from the polymer surface.

## 2.4. AuNP preparation

Synthesis of gold nanoparticles was carried out according to the Brust's method reported in the literature.<sup>62</sup> To a 40.0 ml  $1.0 \times 10^{-3}$  M of tetraoctylammonium bromide solution in toluene, 5.0 ml of aqueous gold chloride solution  $\text{HAuCl}_4$  ( $3.0 \times 10^{-2}$  M) was added in one portion. Then, transfer of metal salt to toluene was observed by color change in toluene which was from colorless to wine red. The mixture was stirred about 2 hours to ensure the transfer of all metal salt to toluene phase. As a reducing agent,  $\text{NaBH}_4$  aqueous solution ( $5.0 \times 10^{-3}$  M, 12.5 ml) was added dropwise while stirring. Solution was allowed to stir for 2 hours. Then, two phases were separated and toluene phase was washed with 0.1M  $\text{H}_2\text{SO}_4$  and 0.1M  $\text{NaOH}$  aqueous solutions; then, dried over  $\text{MgSO}_4$  to obtain gold nanoparticles.

## 2.5. Polymer-Gold Nanoparticle Composite Preparation

Prior to Au NPs-polymer composite sample preparation, polymer films, **PTFT** and **PEFE** (25 mC), were deposited on to ITO electrodes via constant potential electrolysis. Then polymer film coated electrodes were dipped into AuNP solution for different time intervals. To monitor the AuNP deposition due to the interaction between sulphur atoms of the polymer and Au, UV-vis spectra of the polymer coated ITO electrodes were recorded in ACN.

## 2.6. Characterization of Polymer

### 2.6.1. Cyclic Voltammetry (CV)

Cyclic voltammetry is one of the most widely used electroanalytical techniques for acquiring qualitative information about electrochemical reactions because it offers simple usage and well-rounded data. There are three electrodes in the properly working system which are working electrode (WE), reference electrode (RE) and counter electrode (CE). In CV, potentiostat linearly scans the potential of WE, the electrode at which the redox reaction of interest is taking place, with respect to RE. There is a current creation from WE to CE when the potential is applied to the system, and current flow detection is done by potentiostat. Data are then plotted as current ( $i$ ) vs. potential ( $E$ ).

## 2.7. Spectroelectrochemistry

Spectroelectrochemistry combines electrochemical and spectroscopic methods. It provides information about the some changes of transitions in electronic states of CPs between different redox states and information related with  $E_g$  values which form upon doping process of the materials. Spectroelectrochemical studies were done by Hewlett-Packard 8453A diode array UV-vis spectrometer. In these experiments, three electrode system was by application of potential to observe absorption spectra. Pt wire, Ag wire and indium tin oxide (ITO, Delta Tech. 8-12  $\Omega$ , 0.7 cm x 5 cm) were used as CE, pseudo-RE, WE respectively

## 2.8. Kinetic Properties

Kinetic studies make possible to obtain information about optical properties of CPs such as percent transmittance differences ( $\Delta\%T$ ), switching time ( $t_s$ ) and coloration efficiency (CE). In this study,

three electrode system was used as in the SPEL analysis in which Pt wire as CE, a Ag wire as a pseudo-RE and ITO as a WE. Kinetic behaviors of polymers were studied with a Hewlett-Packard 8453A diode array UV-vis spectrometer.

## **2.9. Characterization of Polymer-Gold nanoparticle composites**

### **2.9.1. UV Measurements**

Formation of AuNPs and their interaction with polymer films, **PTFT** and **PEFE**, were monitored by recording their UV-vis spectra in ACN at different time intervals. A Hewlett-Packard 8453A diode array UV-vis

### **2.9.2. Scanning Electron Microscope (SEM)**

The scanning electron microscope (SEM) is a type of technique that uses a focused beam of high-energy electrons instead of light to generate signals at the surface of solid specimens. The signals deriving from electron-sample interactions reveal information about the sample including morphology, chemical composition, and crystalline structure of materials. Detection of gold nanoparticles in composite materials was investigated by the FEI-Quanta 400 FEG scanning electron microscope (SEM) scanning microscope.

## CHAPTER 3

### RESULTS AND DISCUSSION

#### 3.1. Electrochemical Properties of Monomers

##### 3.1.1. Cyclic Voltammograms of Monomers

Prior to polymer synthesis, electrochemical behavior of monomers, **TFT** and **EFE**, were investigated utilizing CV. In the case of **TFT**, 0.1 M TBABF<sub>4</sub> / ACN / DCM mixture was used as electrolytic medium due poor solubility of **TFT** in ACN. On the other hand, DCM/BF<sub>3</sub>O(C<sub>2</sub>H<sub>5</sub>)<sub>2</sub> mixture containing 0.1 M TBAPF<sub>6</sub> was used as solvent-electrolyte mixture for investigating the electrochemical behaviour of **EFE**. The cyclic voltammograms of both monomers are shown in Figure 13. An inspection of Figure 13a and 13b reveals that both monomers exhibit an irreversible oxidation peak, 1.12 V vs. Ag/AgCl and 1.24 V vs Ag/AgCl for **EFE** and **TFT**, respectively, during the anodic scan. Since both monomers have the same electron acceptor unit, which is 9,9- dihexylfluorene, the slight difference in their oxidation potentials can be explained on the basis of electron donating power of donor side groups. Due to the higher electron donating effect of EDOT than thiophene, monomer **EFE** has slightly lower oxidation potential.

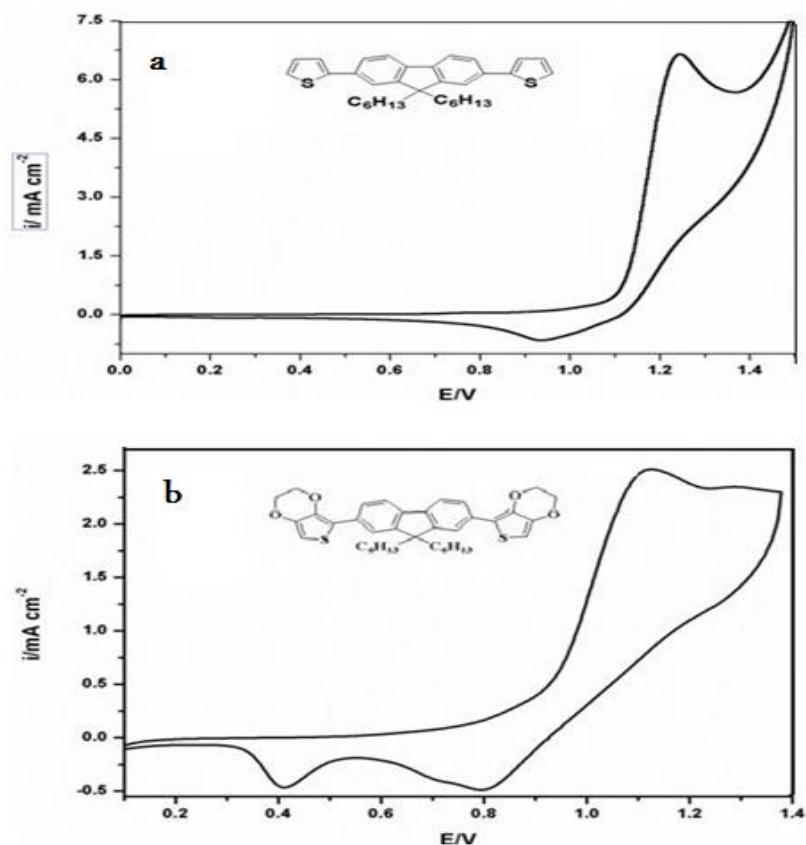


**Figure 13:** Cyclic voltammograms of a) TFT in 0.1 M TBABF<sub>4</sub>/ACN/DCM b) EFE in 0.1 M TBAPF<sub>6</sub>/DCM/BF<sub>3</sub>O(C<sub>2</sub>H<sub>5</sub>)<sub>2</sub> solution at 100 mV/s vs. Ag/AgCl. Concentration of monomers: TFT= 5.0 x10<sup>-3</sup> M, EFE= 4.0 x10<sup>-3</sup>

### 3.1.2. Electropolymerization of Monomers

Monomers are electrochemically polymerized by repetitive cycling in their proper electrolytic medium. Different polymerization media were used in the polymer synthesis due to characteristic solubilities of monomers and polymers. Since solubility of **TFT** was limited in ACN, it was dissolved in minimum amount of DCM before ACN was added. Its polymerization was performed in ACN/DCM (98/2, v/v) solvent mixture containing 0.1 M TBABF<sub>4</sub> as an electrolyte. In the case of **EFE**, polymerization medium was DCM/ BF<sub>3</sub>O (C<sub>2</sub>H<sub>5</sub>)<sub>2</sub> (97/3, v/v) in which TBAPF<sub>6</sub> was used as electrolyte. Polymers, **PTFT** and **PEFE**, were deposited either on Pt or on ITO working electrodes via potential cycling from 0.00 to 1.30 V (for **TFT**) and 0.00 to 1.40 V (for **EFE**). During repetitive cycling, formations of new reversible redox couples were observed at about 1.05 V and 0.9 V for **TFT** and **EFE**, respectively (See Figure 14a and 14b). These newly formed redox couples revealed the electroactive polymer film formation on the surface of working electrode with increasing thickness of polymer film.

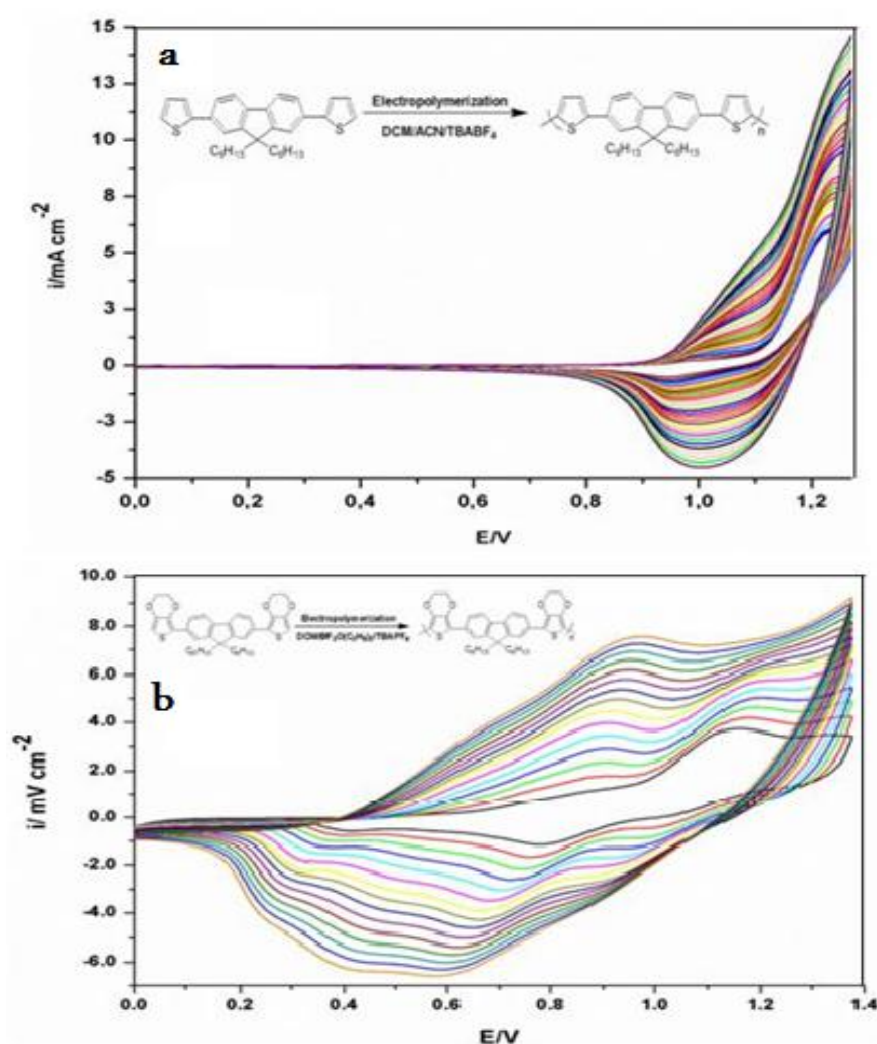


**Figure 14:** Electropolymerization of a)  $5.0 \times 10^{-3}$  M of TFT in ACN/DCM (98/2; v/v) with 0.1M TBABF<sub>4</sub>, b)  $4.0 \times 10^{-3}$  M of EFE in DCM/ BF<sub>3</sub>O(C<sub>2</sub>H<sub>5</sub>)<sub>2</sub> with 0.1 M TBAPF<sub>6</sub> at 100 mV/s (vs. Ag/AgCl)

## 3.2. Characterization of Polymers

### 3.2.1. Electrochemical Properties of Polymers

Investigation of electrochemical behaviors of polymers, **PTFT** and **PEFE**, were performed in 0.1 M TBABF<sub>4</sub> /ACN and TBAPF<sub>6</sub> /ACN, respectively in monomer free solution. As it seen from the cyclic voltammograms shown in Figure 15a, **PTFT** shows a well-defined reversible redox couple at 1.1 V. **PEFE**, on the other hand, exhibits two redox couples at 0.7 V and 1.0 V, due to formation of charge carriers (Figure 15b). Peak currents variation, which is a function of voltage scan rate, was also investigated by recording the cyclic voltammograms of polymer films at different voltage scan rates. The results are depicted in Figure 16. The linear increase in anodic peak current with increasing voltage scan rate indicates not only the existence of polymer film on the working surface with a well adhesion but also a non-diffusional electron transfer process.

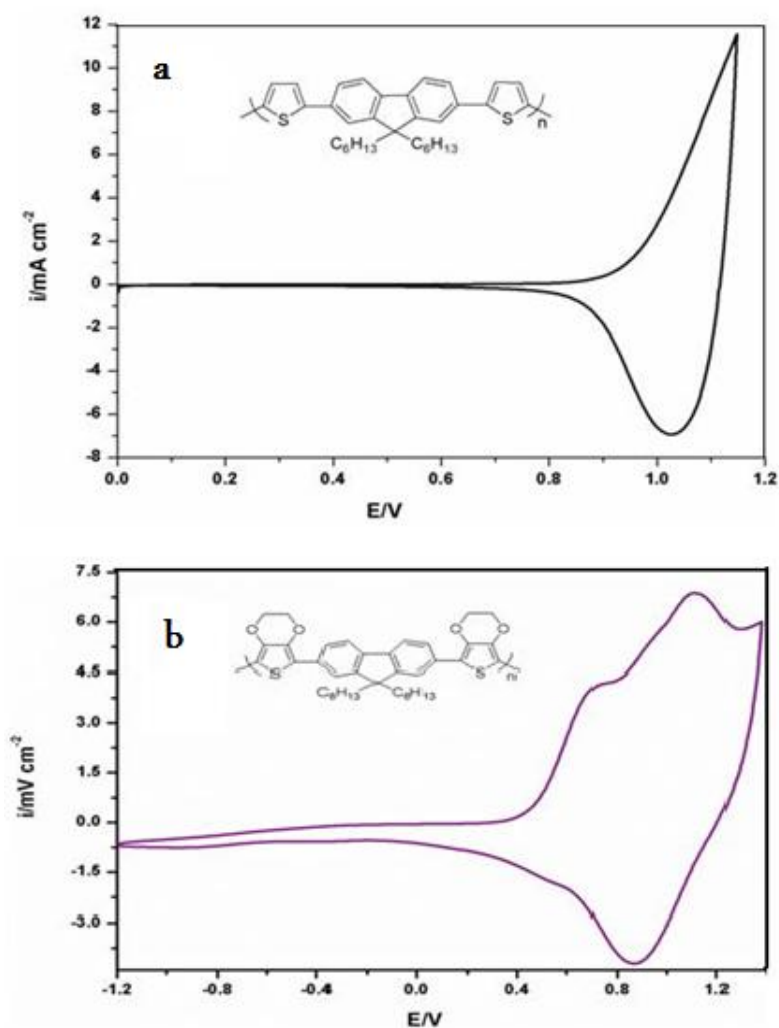


**Figure 15:** Cyclic voltammograms of films a) PTFT in 0.1 M TBABF<sub>4</sub>/ACN b) PEFE in 0.1M TBAPF<sub>6</sub>/ ACN on a Pt disk electrode at 100 mV/s (vs. Ag/AgCl).

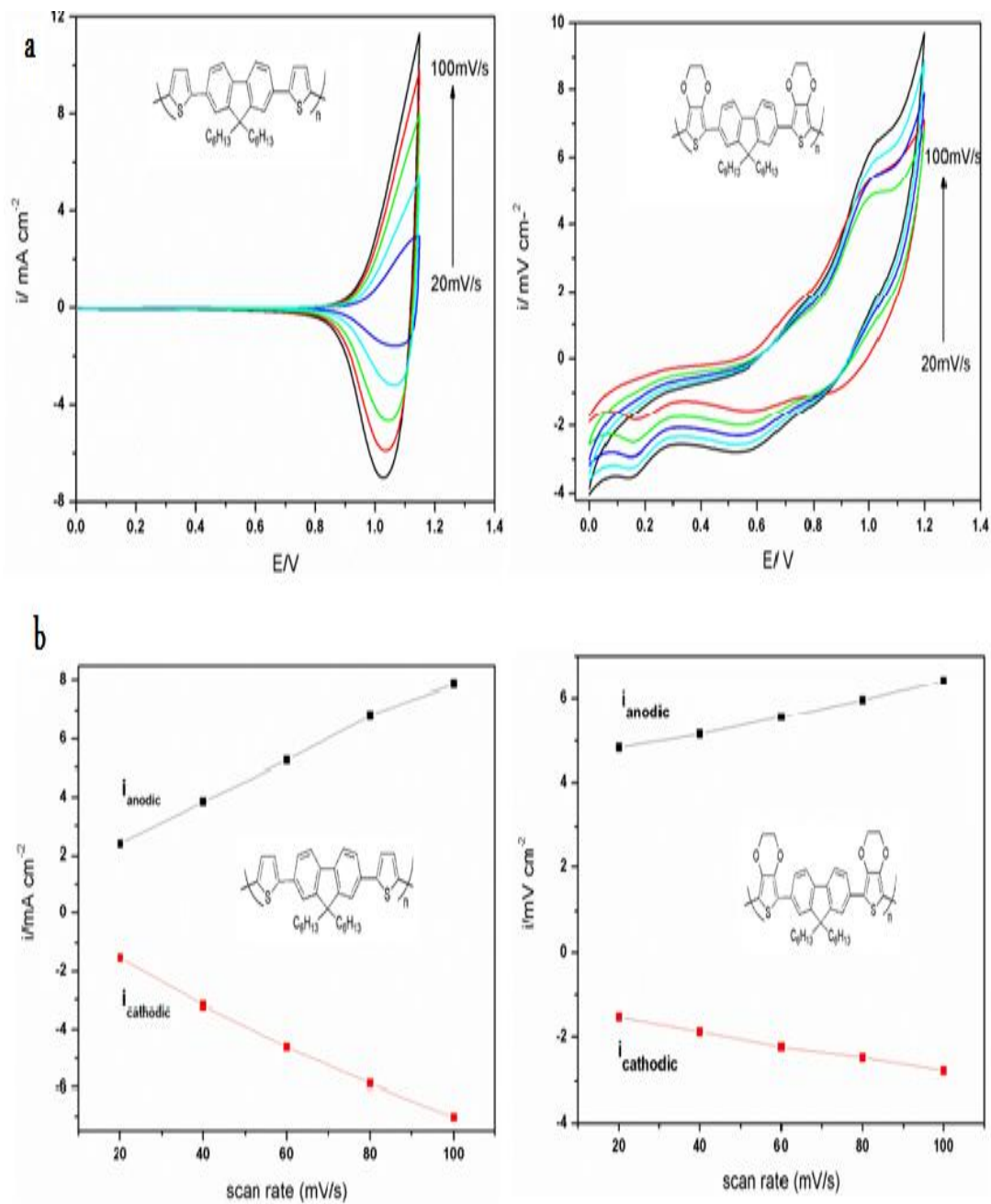


**Figure 16:** (a) Scan rate dependence of **PTFT** and **PEFE** film on a Pt disk electrode in 0.1 M TBABF<sub>4</sub>/ACN and TBAPF<sub>6</sub>/ACN between 20-100 mV/s. (b) Relationship of anodic ( $i_{p,a}$ ) and cathodic ( $i_{p,c}$ ) peaks current as a function of scan rate between to redox states which are neutral and oxidized state

### 3.3. Properties of Composite Materials

#### 3.3.1. UV-Vis Measurements

Since AuNP solution has a characteristic absorption band at around 550 nm, due to plasmon resonance, interaction of AuNP with sulphur containing polymers were investigated by recording their UV-vis absorption spectrum before and after dipping polymer films in AuNP solution and the results are given in Figure 17. Prior to immersing into AuNP particles solution, **PTFT** film exhibits an absorption band at 400 nm due to  $\pi \rightarrow \pi^*$  transition. Upon immersing polymer film coated ITO electrode in AuNP solution for 1 h, a new absorption band at about 550 nm, characteristic of AuNP, was observed indicating the existence of AuNP on the polymer surface. To investigate the effect of contact time with AuNP solution, **PTFT** film was kept in contact for further four hours and UV-vis absorption spectrum was recorded with one hour time intervals. As seen from Figure 17a, the intensity of 550 nm absorption band increases up to three hours and no appreciable increase was observed beyond this point. Thus, 4 h of contact time was assumed to be enough to obtain maximum amount of AuNP on the **PTFT**. Same procedure was applied for the **PEFE** films. As it seen from Figure 17b, before immersing into AuNP solution, **PEFE** has an absorbance band at 475 nm, due to  $\pi \rightarrow \pi^*$  transition. After keeping the polymer film 1 h in contact with AuNP solution, characteristic AuNP band was observed at about 600 nm. This band intensified upon keeping it in contact with AuNP solution for further one hour. However, no appreciable increase in intensity of 600 nm band was noted beyond 2 h contact time. As a result, optimum dipping time in Au NP solution for **PTFT** and **PEFE** are determined as 4h and 2h, respectively.

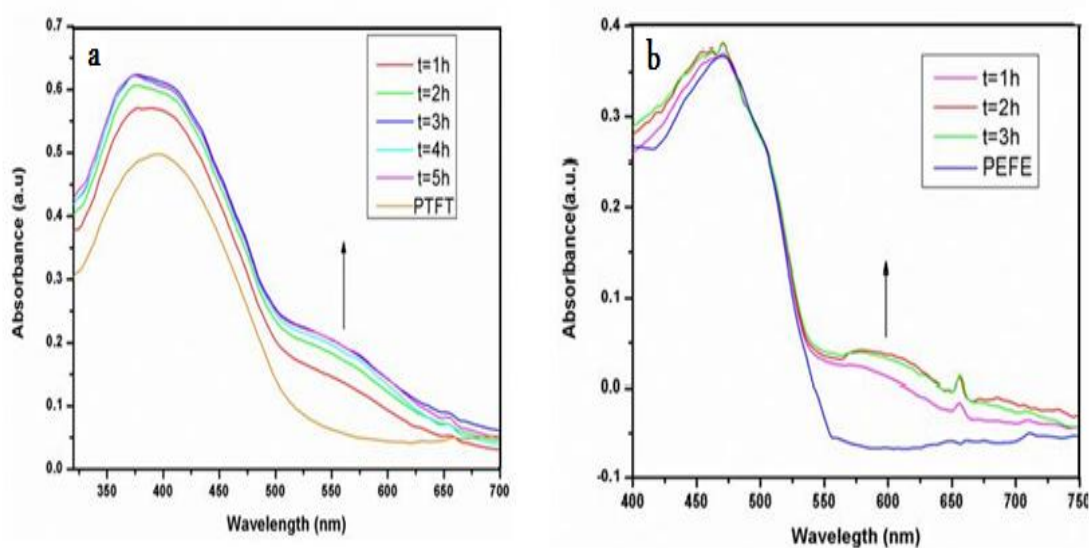


**Figure 17:** UV-vis absorption spectra of a) **PTFT**-AuNPs b) **PEFE**- AuNPs composites in ACN

#### 3.3.2. Scanning Electron Microscope (SEM) Images

In order to find further support for the Au-S interaction on the polymer films, SEM images of **PTFT** and **PEFE** films before and after dipping into AuNP solutions were recorded. To record the images of composite materials, back scattered electrons (BSE) are detected. In this method, electrons which are

reflected or backscattered from the sample are used to create the images. Theoretically, heavy elements back scatter electrons more strongly than the light elements which cause contrast between different areas in the images. As a result, heavy elements are brighter than light elements. In our SEM images, it is expected to observe Au nanoparticles brighter than the polymer films. For **PTFT**-AuNP composite, magnification was 2000 for each image. SEM images of **PTFT** films before and after immersing into AuNP solution are depicted in Figure 18 a-e. Figure 18a, shows the **PTFT** SEM image before the interaction with Au and as it is seen there is no difference in contrast of **PTFT** itself. However, it is obviously seen in Figure 18 b that AuNPs are accumulated onto surface of **PTFT**. Due to the BSE effect, AuNPs are brighter as compared to **PTFT**. Figure 18c, 18d and 18e correspond to 2, 3 and 4 h interaction of **PTFT** with AuNP containing solution. Similar to the results obtained from UV-vis measurements, AuNPs reach to their maximum value within 4 h on the **PTFT**.

The last five SEM images given in Figure 19 belongs to **PEFE** and its composite with AuNP. In this case, magnification value was 20000 for each SEM image. Similar to the SEM image of **PTFT**, **PEFE** also has no contrast difference in itself (See Figure 19a). SEM images change and AuNPs become observable upon keeping **PEFE** film in contact with AuNP solution (See Figure 19 b-e). According to SEM images given in figure 19c, 19d and 19e 2h is sufficient to obtain maximum amount of AuNP on the **PEFE** surface which is consistent with the results obtained from the UV-vis measurements.

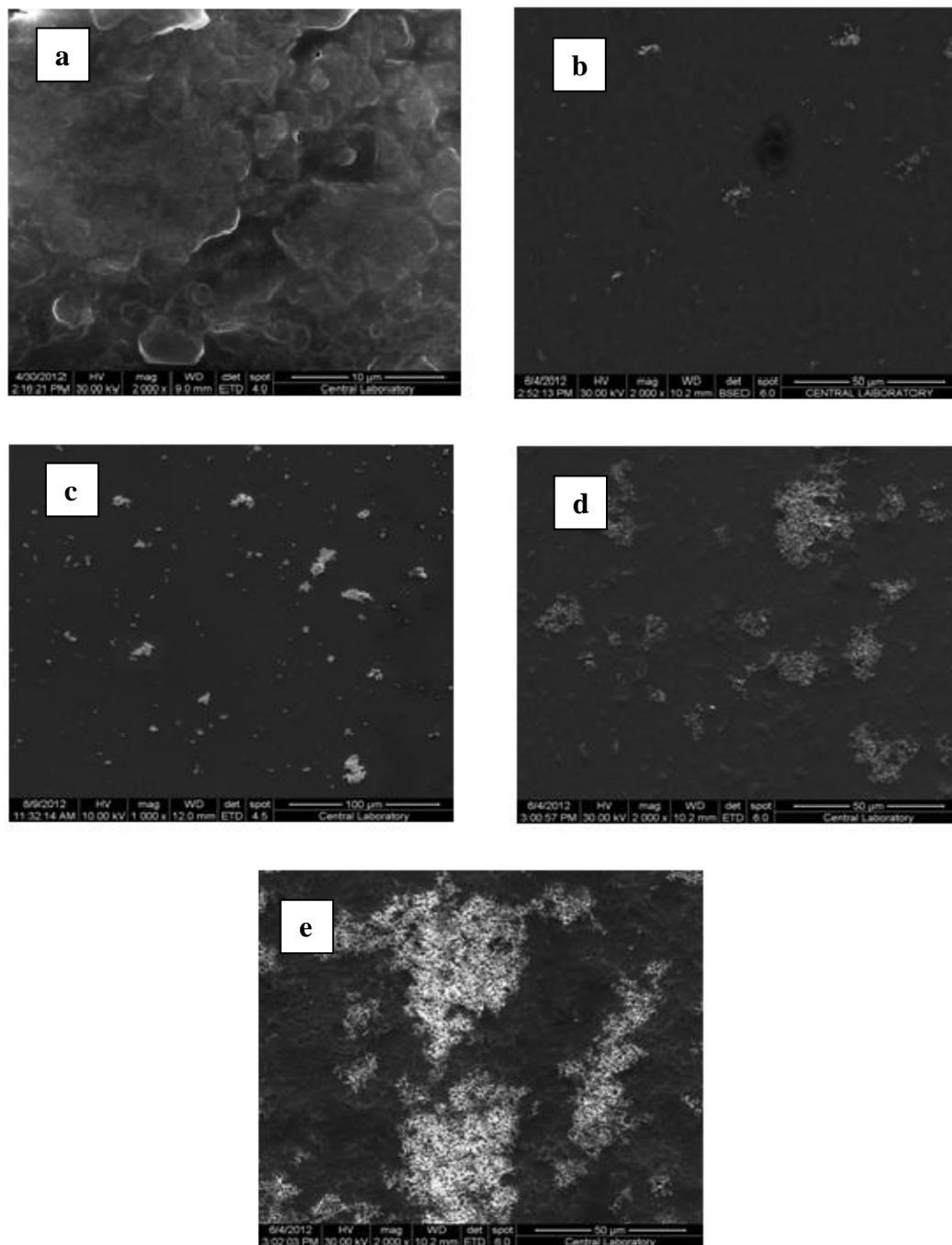


**Figure 18:** SEM images of PTFT and PTFT-AuNP composites with respect to polymer –Au interaction times a) PTFT b) 1h c) 2h d) 3h e) 4h in AuNP solution

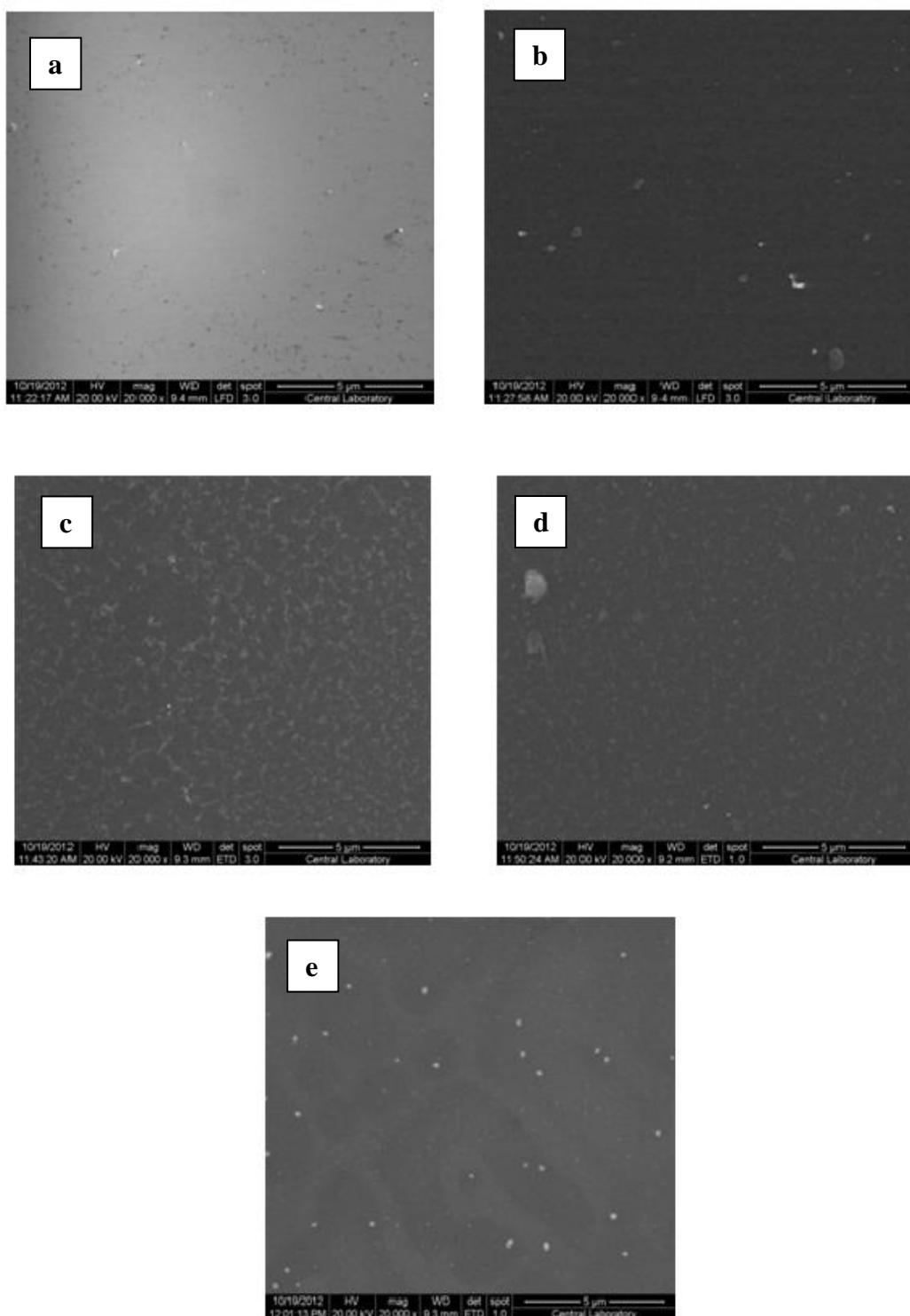


**Figure 19:** SEM images of **PEFE** and **PEFE-AuNP** composites with respect to polymer –Au interaction times a) **PEFE** b) 1h c) 2h d) 3h e) 4h in AuNP solution

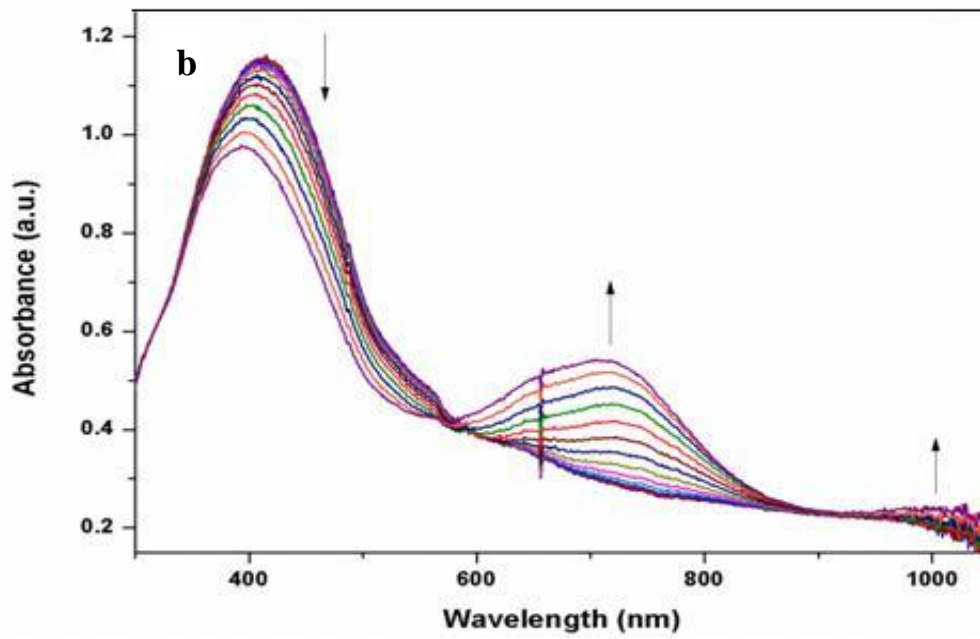
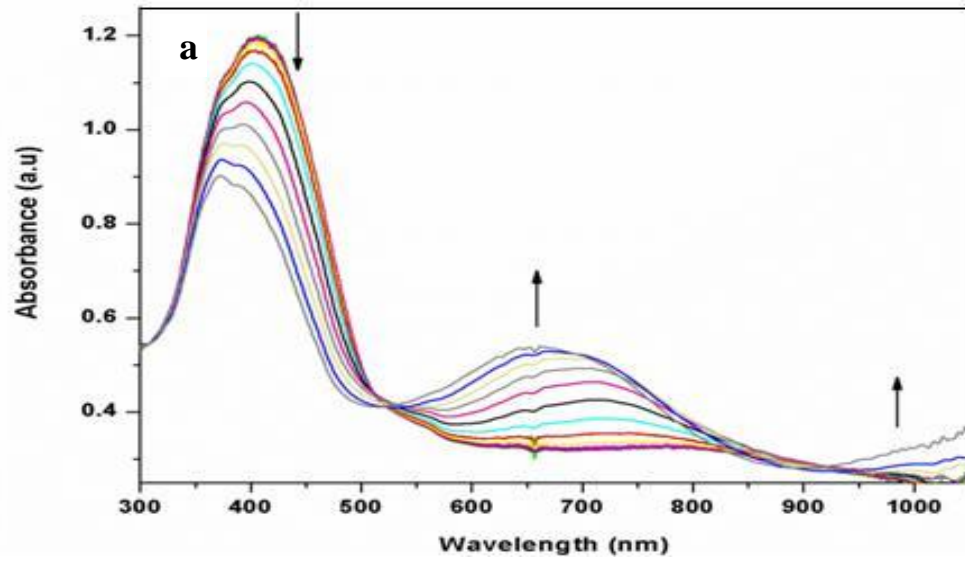
### 3.4. Comparison of Polymer-Au NP composites

#### 3.4.1. Comparison of Spectroelectrochemical Properties of Polymers and Composites

Spectroelectrochemical (SPEL) data reveals the electro-optical properties of the polymers and composite materials that one can observe changes in the electronic absorption spectra under a voltage pulse in a monomer free electrolyte solution via constant potential electrolysis. Neutral form of **PTFT** film has an absorption band at about 400 nm and **PEFE** has at about 350 and 450 nm shown in Figure 20. These neutral absorption bands correspond to  $\pi$ - $\pi^*$  transition of the polymers. However, these absorption bands lose their intensity upon oxidation and new band formations are observed for both polymer films. In the case of **PTFT**, there are new band formations at about 725 nm and upon further oxidation at 1000 nm which indicates the formation of new charge carriers. **PEFE** has similar SPEL data with the previous polymer **PTFT**. Its valance band -conduction band transition at 350 and 450 nm diminish during oxidation and a new band starts to form at about 600 nm. Upon further oxidation, formation of a weak and broad band which is around 940 nm is also observed. Both polymers also show electrochromic responses between oxidized and reduced forms. **PTFT** film is yellow colored in the neutral state and dark green in its oxidized states. For **PEFE**, color changes from yellow to parlament blue as going from its neutral to oxidized state.

In the case of **PTFT**-AuNP composite film, there exist an absorption band due to AuNP besides the 400 nm  $\pi$ - $\pi^*$  transition band of polymer film. Upon oxidation, composite exhibits an absorption band at about 750 nm. This polaron band is red shifted about 25 nm compared to polaron band of **PTFT**. Also, composite has a clear isosbestic point at 590 nm. In the case of **PEFE**-AuNP composite, the absorption band due to AuNP was observed at about 570 nm in its neutral form. Similar to **PTFT**-AuNP composite, isosbestic point of this composite is well-defined and observed at about 520 nm.

The band gap values of polymers **PTFT**, **PEFE** and their composites **PTFT**-AuNP and **PEFE**-Au NP were also determined. These values are calculated as 2.36 eV and 2.26 eV for **PTFT** and **PEFE** and 2.24 eV and 2.21 eV for **PTFT**-AuNP and **PEFE**-AuNP composites, respectively.



**Şekil 20:** Optical absorption spectra of a) PTFT on ITO b) Optical absorption spectra of PTFT-AuNP composites on ITO electrode electrode in 0.1 M TBABF<sub>4</sub>/ACN at potential range between 0.0V and 1.20V.

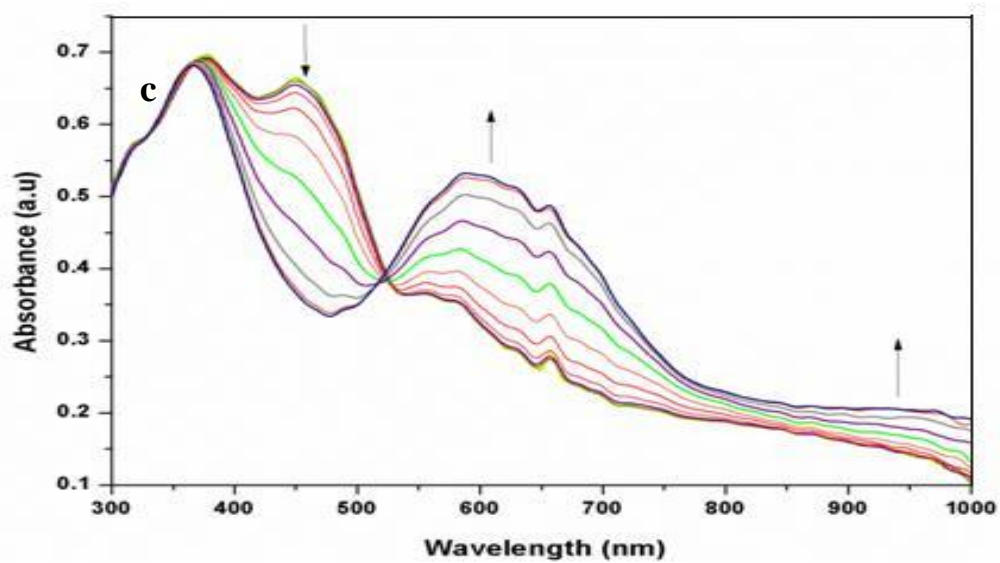
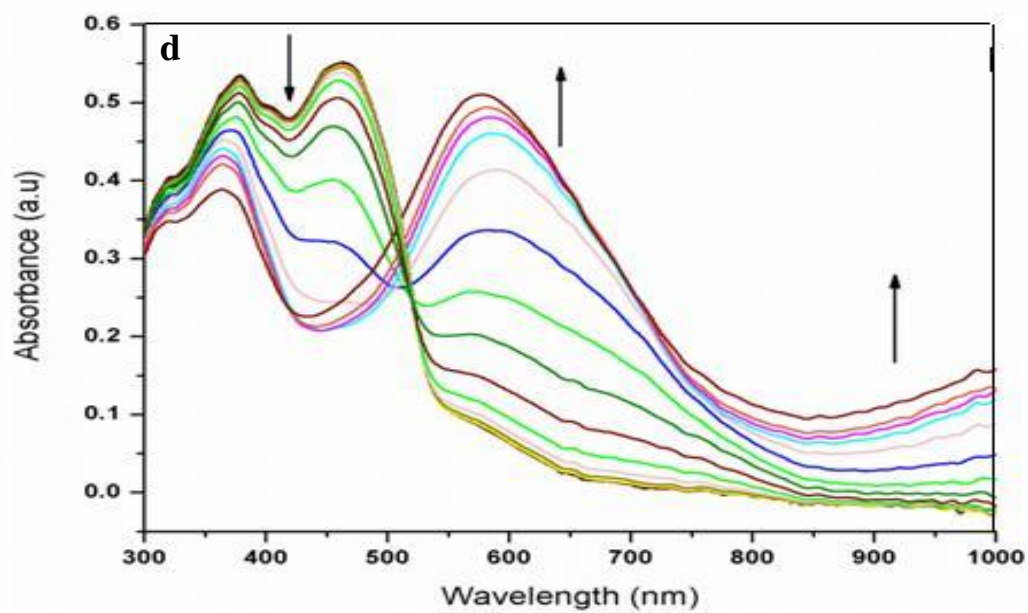


**Figure 21:** Optical absorption spectra of c) **PEFE** on ITO electrode d) **PEFE-AuNP** composites on ITO electrode in 0.1 M TBAPF<sub>6</sub>/ACN at potential range between 0.0V and

**Table 1:** Colors of the **PTFT**, **PEFE** on ITO electrodes in their neutral and oxidized state

	<b>PTFT</b>	<b>PEFE</b>
<b>Neutral State</b>		
<b>Oxidized State</b>		

### 3.4.2. Comparison of Kinetic Properties of Polymers and Composites

Comparison of polymers and composite materials regarding their kinetic properties is one of the beneficial ways to investigate AuNP effect on polymer. Due to its importance in electrochromic applications, investigation of switching times and optical contrast of the polymers and their composites on ITO were also done under square wave input of 0.0 V and 1.25 V for **PTFT** and 0.0 V and 1.23 V for **PEFE** in 10 s intervals by monitoring the visible transmittance and the results are tabulated in Table 2. As seen from Table 2, the percent transmittance ( $\Delta\%T$ ) between the neutral and oxidized states of **PTFT** film was found to be 16.71% and it decreases to 6.59% for its composite at 470 nm. Same effect was also observed for **PEFE**. **PEFE** has a value of percent transmittance % 27.72 between its neutral and oxidized states at 460 nm. When Au is adsorbed on the polymer surface, % transmittance decreases to 23.22%. Thus, it can be clearly concluded that AuNP has a negative effect on transmittance values of the polymers.

On the other hand, time required for change in redox states of both polymers has improved after Au-S interaction. That is, **PTFT**/Au composite can oxidize more quickly which is about one third of the **PTFT**'s oxidation time. Similarly, oxidation time of **PEFE** dropped from 2.19 s to 1.94 s after composite preparation.

The other parameter for electrochromic applications is the coloration efficiency values of the polymer. The CE were found to be 503.9 cm<sup>2</sup>/C at 470 nm for **PTFT** film, 1050.0 cm<sup>2</sup>/C at 460 nm for **PEFE** film. These relatively high CE value of polymers unfortunately, decreased to 75.4 and 148.7 cm<sup>2</sup>/C for **PTFT**/Au and **PEFE**/Au composites, respectively.

**Table 2:** Optical and electrochemical properties of **PTFT**, **PEFE**, **PTFT**/AuNP and **PEFE**/ AuNP composites.

	<b>PTFT</b>	<b>PEFE</b>	<b>PTFT</b> -Au NP composite	<b>PEFE</b> -Au NP composite
E <sub>m</sub> <sup>ox</sup> (V)	1.12	1.24	-	-
λ <sub>max</sub> (nm)	470	370 460	550 shld. 470	600 shld. 370 460
E <sub>g</sub> (eV)	2.36	2.26	2.24	2.21
Δ%T	16.71	27.72	6.59	23.22
Color	Yellow (neutral) Dark green (oxidized)	Yellow (neutral) Parliament blue (oxidized)	-	-
t <sub>s</sub> (s)	0.83	2.19	0.34	1.94
CE <sub>95%</sub> (cm <sup>2</sup> /C)	503.9	1050.0	75.4	148.7

### 3.4.3. Comparison of Fluorescence Properties of Polymers and Composites

Fluorescence is the emission of light by a substance that has absorbed light or other electromagnetic radiation. The emitted light has a longer wavelength, and therefore lower energy, than the absorbed radiation. Since both polymers synthesized in this work, **PTFT** and **PEFE**, are polyfluorene derivatives with blue light emission, we have also investigated the effect of AuNP on the fluorescence emissions of both polymers. For this purpose **PTFT** and **PTFT**-AuNP composite were dissolved in toluene and these solutions were excited at 353 nm. Emission spectra were recorded between 375 nm and 700 nm and the results are given in Figure 21. As it could be seen from Figure 21a, **PTFT** solution has maximum emission intensity at about 400 nm and 500 nm. (λ<sub>max</sub> = 492 nm). However, after immersing it in AuNP solution, there is a significant decrease in the emission intensity of 500 nm emission band of **PTFT**. It is clearly seen that AuNPs have quenching effect on the polymer fluorescence intensity. Similar results were obtained for the **PEFE** and **PEFE**-AuNP composite fluorescence spectra. Firstly, **PEFE** and **PEFE**-AuNP composite were dissolved in toluene. Both solutions were excited at 360 nm and their emission spectra were recorded in 400-600 nm region. An inspection of figure 21b indicates that **PEFE** emits light with a maximum intensity at about 400-450 nm (λ<sub>max</sub> = 417 nm), however, a quenching effect was also noted for **PEFE**-AuNP composite material. In Table 3, quenching effect of AuNPs on fluorescence emissions of polymers could be clearly observed.

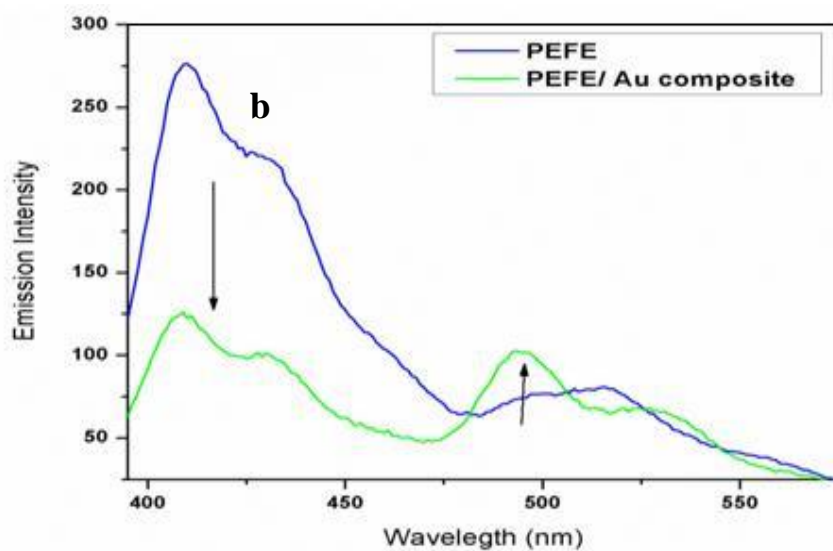
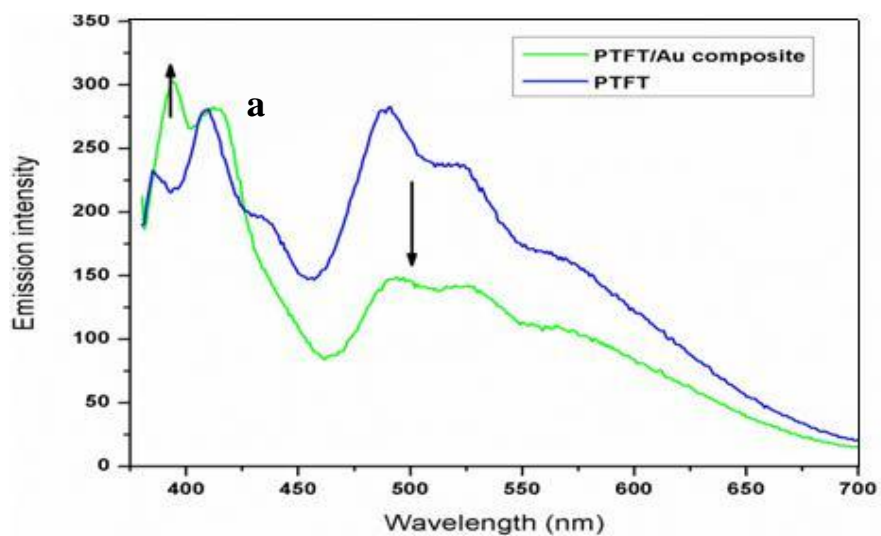


**Figure 22:** Fluorescence spectra of a) **PTFT** and **PTFT/ AuNP** composite b) **PEFE** and **PEFE/ AuNP** composite solution in toluene at room temperature

**Table 3:** Fluorescence emissions of PTFT, PEFE, PTFT/AuNP, PEFE/ AuNP composites in toluene

	<b>PTFT</b>	<b>PEFE</b>
<b>Polymer</b>		
<b>Composite</b>		



## CHAPTER 4

### CONCLUSION

In this study, syntheses of two new monomers; 2-(9,9-dihexyl-2-(thiophen-2-yl)-9H-fluoren-7-yl)thiophene (TFT) and 5-(9,9-dihexyl-2-(2,3-dihydrothieno[3,4-b][1,4]dioxin-5-yl)-9H-fluoren-7-yl)-2,3-dihydrothieno[3,4-b][1,4] dioxine (EFE) were successfully achieved. Then, monomer characterizations were done by spectroscopic techniques ( $^1\text{H}$  NMR,  $^{13}\text{C}$  NMR and FTIR). Additionally, syntheses of polymers, **PTFT** and **PEFE**, were achieved by common electrochemical methods which are potential cycling and constant potential electrolysis. These monomers were characterized with cyclic voltammetry and UV-vis spectrometry.

In the second part of the study, Au NPs were synthesized and polymer-Au NP composites prepared by dipping polymer coated ITOs into the AuNP solution with different time intervals. Deposition of AuNP onto polymer surface was controlled with UV-vis spectrometer, which gives signal due to surface plasmon resonance. Deposition of AuNPs was also proved by SEM according to different dipping time of polymers in Au NP solution. After that, polymer and their composites were compared regarding their optical and fluorescence properties.

According to optical results, AuNPs have mostly negative effect on polymer properties. CE and  $\Delta\%T$  values reduce for composites of both polymers **PTFT** and **PEFE**. Although **PTFT** and **PEFE** have relatively high CE values, which are 503.9 and 1050.0  $\text{cm}^2/\text{C}$ , respectively, their composites have lower CE values.  $\Delta\%T$  values were found to be low for both polymers and their composites. However, both polymers exhibit relatively shorter switching time values after Au adsorbed on the polymer surface. Also, a slight decrease in the band gap values ( $E_g$ ) of polymers were observed after composite preparation.  $E_g$  values drops from 2.36eV to 2.24eV for **PTFT** and, from 2.26eV to 2.21eV for **PEFE**.

Fluorescence results indicated that AuNP have quenching effect on the emission intensities of **PEFE** and **PTFT**. There is a significant decrease in the emission intensity of **PTFT** at 500 nm after AuNP interaction. Similar results were obtained for the **PEFE** fluorescence emission intensity. There is a decrease of the maximum emission intensity about 425 nm indicating AuNP quenched its emission.



## REFERENCES

1. C. K. Chiang, C. R. Fincher, Y. W. Park, A. J. Heeger, H. Shirakawa, E. J. Louis, S. C. Gau, A. G. MacDiarmid, *Phys. Rev. Lett.*, 39, 1089 -1977.
2. A. J. Heeger, *Angew. Chem. Int. Ed.*, 2001, 40 (14), 2591.
3. A. J. Heeger, *Synth. Met.*, 2002, 125 (1), 23.
4. A. J. Heeger, S. Kivelson, R. J. Schrieffer, W. P. Su, *Rev. Mod. Phys.*, 1988, 60, 78.
5. A. G. MacDiarmid, and A. J. Epstein, *Synth. Met.*, 1994, 65, 103.
6. J. F. Morin, M. Leclerc, *Macromolecules*, 2001, 34, 4680.
7. J. H. Burroughes, D. D. C. Bradley, A. R. Brown, R. N. Marks, H. Friend, P. L. Burns, and A. B. Holmes, *Nature*, 1990, 347, 539.
8. P. K. H. Ho, D. S. Thomas, R. H. Friend, and N. Tessler, *Science* 1999, 285, 233.
9. H. Koezuka, and A. Tsumura, *Synth. Met.*, 1989, 28, c753
10. j. Miasik, A. Hooper, and B. C. Tofield, *J. Chem. Soc. Farad. Trans. Phys. Chem. in Cond. Pha.*, 1986, 82, 1117.
11. R. G. Mortimer, *Chem. Soc. Rev.*, 1997, 26, 147.
12. J. Roncali, *Chem. Rev.*, 1992, 92, 711.
13. J. H. Burroughes, D. D. C. Bradley, A. R. Brown, R. N. Marks, H. Friend, P. L. Burns, and A. B. Holmes, *Nature*, 1990, 347, 539.
14. (a) P. K. H. Ho, D. S. Thomas, R. H. Friend, and N. Tessler, *Science* 1999, 285, 233.; (b) I. Schwendeman, R. Hickman, G. Sonmez, P. Schottland, K. Zong, D. M. Welsh, and J. R. Reynolds, *Chem. Mater.*, 2002, 14, 3118.
15. N. S. Sariciftci, L. Smilowitz, A. J. Heeger, and F. Wudl, *Science* 1992, 258 1474.
16. H. Koezuka, and A. Tsumura, *Synth. Met.*, 1989, 28, C753.
17. R. G. Mortimer, *Chem. Soc. Rev.*, 1997, 26, 147.
18. J. Tanguay, M. Slama, M. Hoalet, and j. L. Baudouin, *Synth. Met.*, 1989, 28, 145.
19. M. Fukuda, K. Sawada, and K. Yoshino, *J. Polym. Sci., Part A: Polym. Chem.*, 1993, 31, 2465-2472.
20. M. Pomerantz, *Handbook of Conducting Polymers*; 2nd ed. T. A. Skotheim, R. L. Elsenbaumer, J. R. Reynolds, Ed: Marcel Dekker: New York, 1998, 227.
21. I. Schwendeman, *PhD Thesis*, University of Florida, 2002.
22. Cortés, M.; Moreno, *J. C. J. Chem. Educ.*, 2005, 82, 1372.
23. Sadik, A. O.; Brenda, S.; Joasil, P.; Lord, *J. J. Chem. Educ.*, 1999, 76, 967.
24. Bunting, R. K.; Swarat, K.; Yan, D.; Finello, D. *J. Chem. Educ.*, 1997, 74, 421.
25. Lewis, T. W.; Wallace, G. G. *J. Chem. Educ.*, 1997, 74, 703.
26. J. Roncali, *Chem. Rev.*, 1992, 92, 711.
27. G. Zotti, *Handbook of Organic Conductive Molecules and Polymers*, ed. H. S. Nalwa, Wiley, Chichester, 1997, 2, Ch. 4.
28. G. Zotti, *Handbook of Organic Conductive Molecules and Polymers*, ed. H. S. Nalwa, Wiley, Chichester, 1997, Vol. 2, Ch. 4.
29. J. R. Reynolds, S. G. Hsu, and H. J. Arnott, *J. Polym. Sci Part B Polym. Phys.*, 1989, 27, 2081.
30. S. Asavapiriyonont, G. K. Chandler, G. A. Pletcher, and D. Gunawardena, *J. Electroanal. Chem.*, 1984, 177, 229.
31. E. Genius, G. Bidan, and A. F. Diaz, *J. Electroanal. Chem.*, 1983, 149, 113.
32. C. L. Gaupp, PhD thesis, University of Florida, 2002.
33. D. Sainova, T. Miteva, H. G. Nothofer, U. Scherf, I. Glowacki, H. Fujikawa, and D. Neher, *Appl. Phys. Lett.*, 2000, 76, 1810.
34. A. W. Grice, D. D. C. Bradley, M. T. Bernius, M. Inbasekaran, W. W. Wu, and E. P. Woo, *Appl. Phys. Lett.*, 1998, 73, 629.
35. V. N. Bliznyuk, S. A. Carter, J. C. Scott, G. Miller, *Macromolecules*, 1999, 32, 361.
36. N. Fomina, PhD thesis, University of Southern California, 2009.
37. N. Fomina, PhD thesis, University of Southern California, 2009.

38. M. Fukuda, K. Sawada, and K. Yoshino, *Jpn. J. Appl. Phys., Part 1* 1989, 28, 1433-1435.
39. M. Fukuda, K. Sawada, and K. Yoshino, *J. Polym. Sci., Part A: Polym. Chem.*, 1993, 31, 2465-2472.
40. M. Ranger, D. Rondeau, M. Leclerc; *Macromolecules*, 1997, 30, 7686.
41. J.H. Lee, H.J. Cho, N.S. Cho, D.H. Hwang, J.M. Kang, E.H. Lim, I.J. Lee, H.K. Shim, *J. Polym. Sci. Part A: Polym. Chem.*, 2006, 44, 2943.
42. I. Prieto, J. Teetsov, M.A. Fox, D.A.V. Bout, A.J. Bard, *J. Phys. Chem.*; 2001, 10,5520
43. J. Teetsov, D.A.V. Bout, *J. Phys. Chem. B* , 2000, 104,9378.
44. M. Fukuda,; K. Sawada, K.Yoshino, *J Polym Sci Part A:Polym Chem* 1993, 31, 2465.
45. B. B. Çarbaş., A. Kıvrak , A. M. Önal,*Electrochimica Acta*, 2011, 58, 223– 230
46. S. Akoudad, J. Roncali, *Chem. Commun.* 1998, 12, 2081.
47. A. Güneş, A. Cihaner, and A.M Önal., *Electrochimica Acta*, 2013, 89, 339– 345.
48. B.B. Çarbaş, A. M. Önal, *Electrochimica Acta*, 2012, 66, 38– 44.
49. B. B. Çarbaş, A. Kıvrak, M. Zora, A. M Önal, *React. And Func. Polymers*, 2011, 71,579-587.
50. B. B. Çarbaş., A Kıvrak, M. Zora, A. M. Önal, *J Electroanal Chem.* ,2012,9, 677-680
51. U. Kreibig,; M Vollmer., *Optical Properties of Metal Clusters*; Springer: Berlin, 1995.
52. Schmid, G. *Clusters and Colloids - From Theory to Applications*; VCH: Weinheim, Germany, 1994.
53. S. K. Ghosh,; S. Kundu,; M. Mandal; T. Pal,*Langmuir* 2002, 18,8756.
54. S. K. Ghosh,; T. Pal,; S. Kundu,; S. Nath,; T. Pal,*Chem. Phys. Lett.*2004, 395, 366.
55. S. K. Ghosh,; A. Pal,; S. Kundu,; S. Nath,; S. Panigrahi,; T. Pal, *Chem. Phys. Lett.* 2005, 412,5.
56. R. Kubo, *J. Phys. Soc. Jpn.* 1962, 17, 975.
57. J. D. Jackson,*Classical Electrodynamics*; Wiley: New York, 1975;p 98
58. A. Chaubey, K.K. Pande and B.D. Malhotra, *Anal. Sci.* 2003, 9, 1477–1480.
59. K. Mallick, M.J. Witcomb, A. Dinsmore and M.S. Scurrrell, *Langmuir*, 2005, 21, 7964–7967.
60. S. Efrima, H Metiu., *J. Chem. Phys.* 1979, 70, 1602.
61. P. K Aravind, H Metiu, *Chem. Phys. Lett.* 1980, 74, 301.
62. J. I. Gersten,; A. Nitzan,*J. Chem. Phys.* 1980, 73, 3023.
63. D.-S. Wang,; H. Chew,; M Kerker., *Appl. Opt.* 1980, 19, 2256.
64. C. A. Mirkin,; M. Ratner, *A. Ann. .ReV. Phys. Chem.* 1997, 101,1593.
65. M. A. Rampi; O. J. A Schueller, G. M. Whitesides, *Appl. Phys.Lett.* 1998, 72, 1781.
66. Lanqbein, D. *Theory of Van der Walls Interactions*; Springer: NewYork, 1974.
67. P. K. Jain, K. S. Lee, I. H. El-Sayed and M. A. El-Sayed, *J. Phys.Chem. B*, 2006, 110, 7238–7248;
68. S. Eustis and M. A. El-Sayed, *Chem. Soc. Rev.*, 2006, 35, 209–217;
69. S. Link and M. A. El-Sayed, *J. Phys. Chem. B*, 1999, 103, 4212–4217.
70. K. H. Su, Q. H. Wei, X. Zhang, J. J. Mock, D. R. Smith andS. Schultz, *Nano Lett.*, 2003, 3, 1087–1090.
71. Retrieved from <http://nanocomposix.com/kb/gold/optical-properties> at January, 10 2013
72. R. D. Rauh, and S. F. Cogan, *Solid State Ionics*, 1988, 28-30, 1707.
73. K. Bange, and T. Bambke, *Adv. Mater.*, 1990, 2, 10.
74. A. Dodabalapur, L. Torsi, and H. E. Katz, *Science*, 1995, 268, 270.
75. , M. A Santos, M. A. Esteves, M. C. Vaz, , J. J.R. Silva da Frausto; B. Noszal; E Farkas, *J. Chem. Soc., Perkin Trans.* 1997, 2, 1977
76. O. Stenzel,; A. Stendal,; A. C Voigtsberger, *Sol. Energy Mater. Sol.Cells* 1995, 37, 337.
77. S.Huh and S. B. Kim *J. Phys. Chem. C* 2010, 114, 2880–2885.
78. G. Heywang, and F. Jonas, *Adv. Mater.*, 1992, 4, 116.
79. J Groenendaal, B. L., F. Jonas,, D. Freitag and J. R. Reynolds, *Adv. Mater.*,2000, 12(7), 481.
80. J. Turkevich, P. C. Stevenson and J. Hillier, *Discuss. Faraday Soc.*, 1951, 11, 55–75.
81. J. C. Love, L. A. Estroff, J. K. Kriebel, R. G. Nuzzo andG. M. Whitesides, *Chem. Rev.*, 2005, 105, 1103–1169.
82. R. J. Tseng,; J. Huang,; J. Ouyang,; B. Richard,; R. B. Kaner,; Y. Yang, *Nano Lett.* 2005, 5, 1077–1080.
83. G. Majumdar,; M. Goswami,; T. K. Sarma,; A. Paul,; A. Chattopadhyay, *Langmuir* 2005, 21, 1663–1667.

84. M. M. Oliveira; E. G. Castro; C. D. Canestraro; D. Zanchet; D. Ugarte; L. S. Roman; A. J. G. Zarbin, *J. Phys. Chem. B* 2006, *110*, 17063–17069.
85. C. T. Hable; M. S. Wrighton, *Langmuir* 1991, *7*, 1305–1309.
86. K.C. Graber, K.J. Allison, B.E. Baker, R.M. Bright, K.R. Brown, G. Freeman, A.P. Fox, C.D. Keating, M.D. Musick, M.J. Natan, *Langmuir*, 1996, *12*, 2353.
87. M.D. Musick, D.J. Pena, S.L. Botsko, T.M. McEvoy, J.N. Richardson, M.J. Natan, *Langmuir*, 1999, *15*, 844.
88. S. Bharathi, M. Nogami, S. Ikeda, *Langmuir*, 2001, *17*, 1.

## APPENDIX A

### NUCLEAR MAGNETIC RESONANCE SPECTRA OF TFT AND EFE MONOMERS

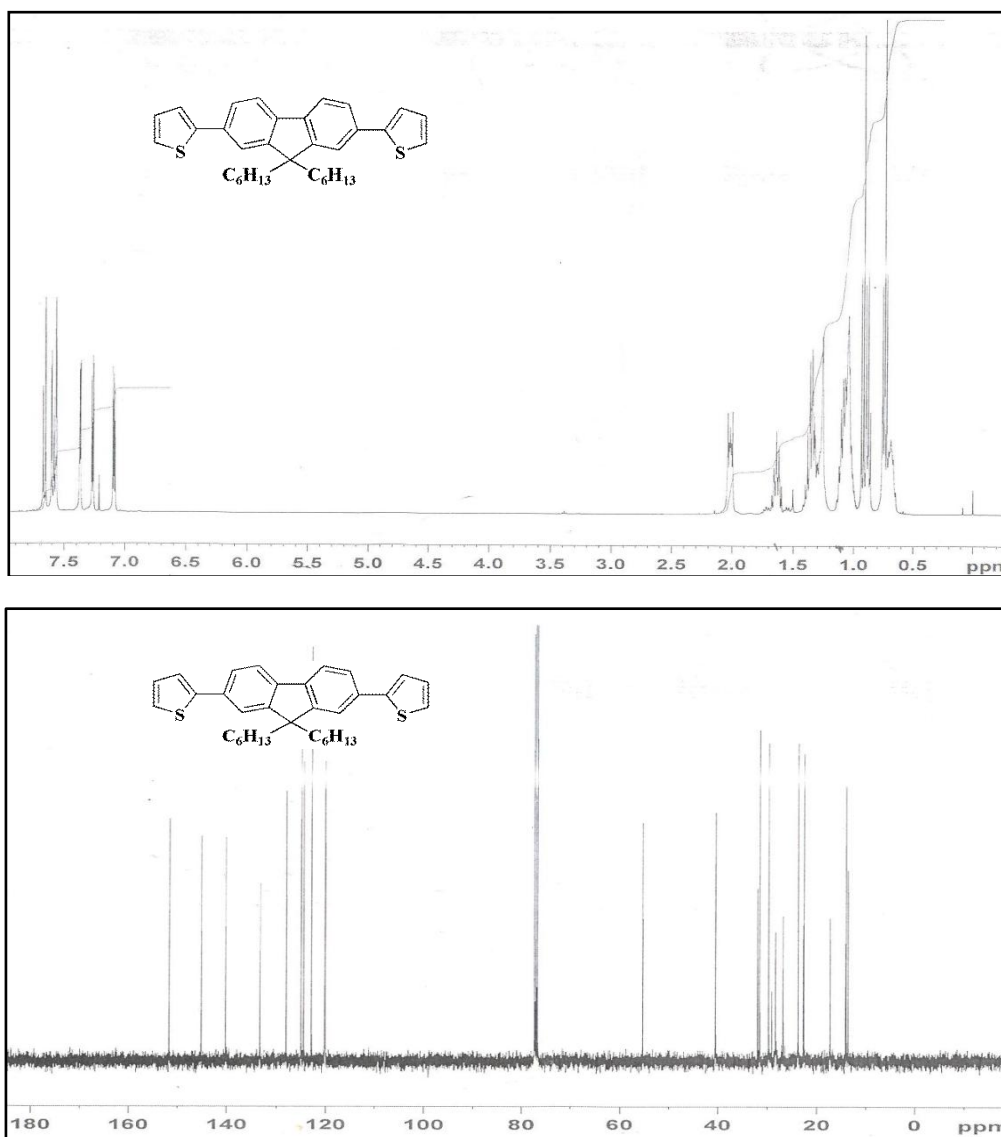


Figure A.1.  $^1\text{H}$  NMR and  $^{13}\text{C}$  NMR of TFT monomer

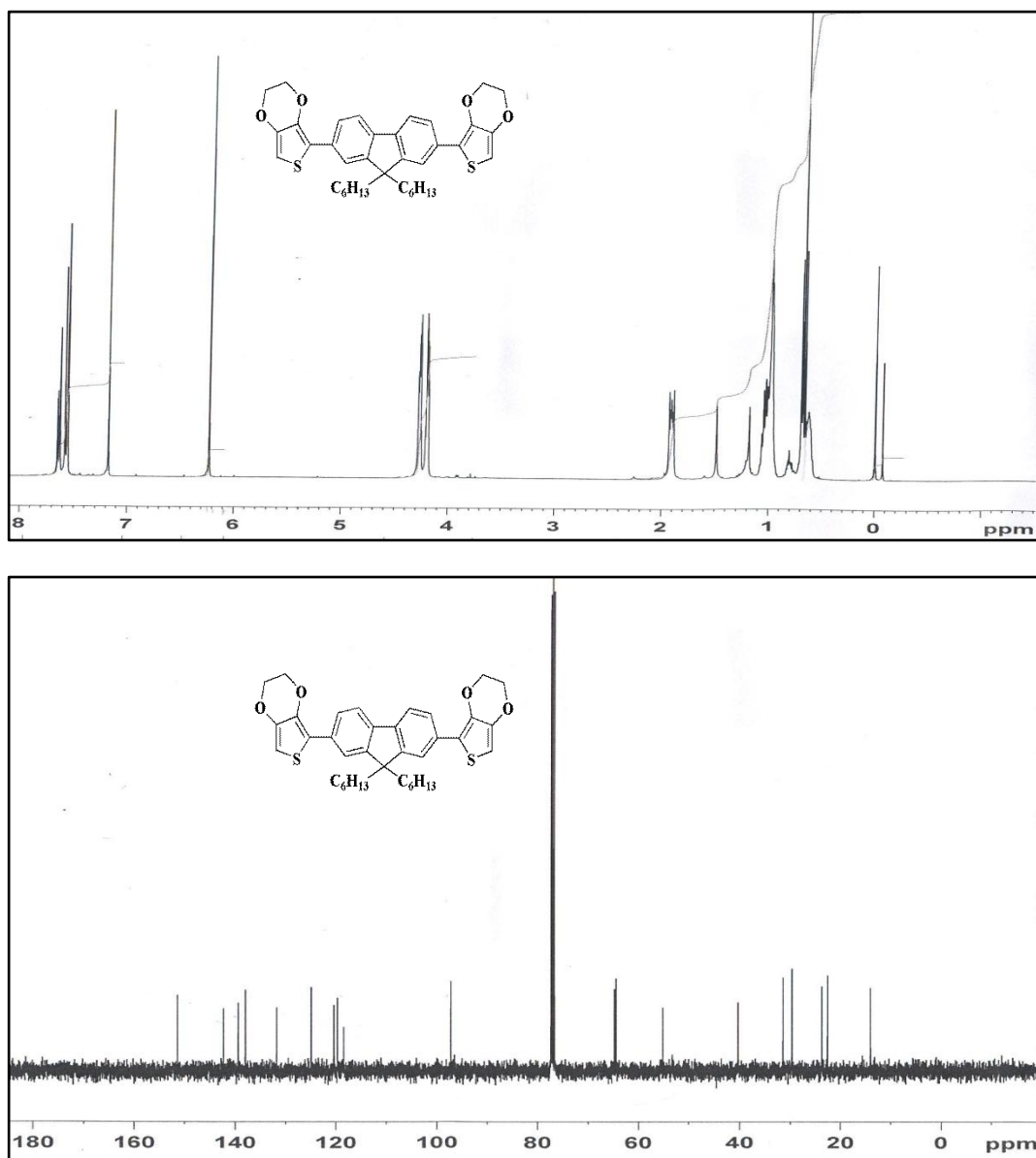


Figure A.2. <sup>1</sup>H NMR and <sup>13</sup>C NMR of EFE monomer

## APPENDIX B

### FTIR SPECTRA OF MONOMERS AND POLYMERS

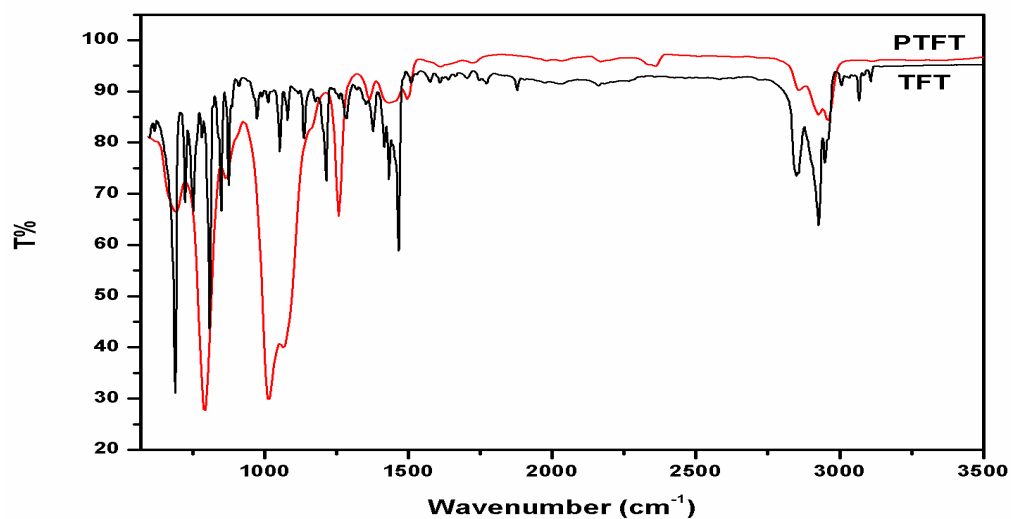


Figure B.1. FTIR spectrum for monomer **TFT** and its polymer **PTFT**

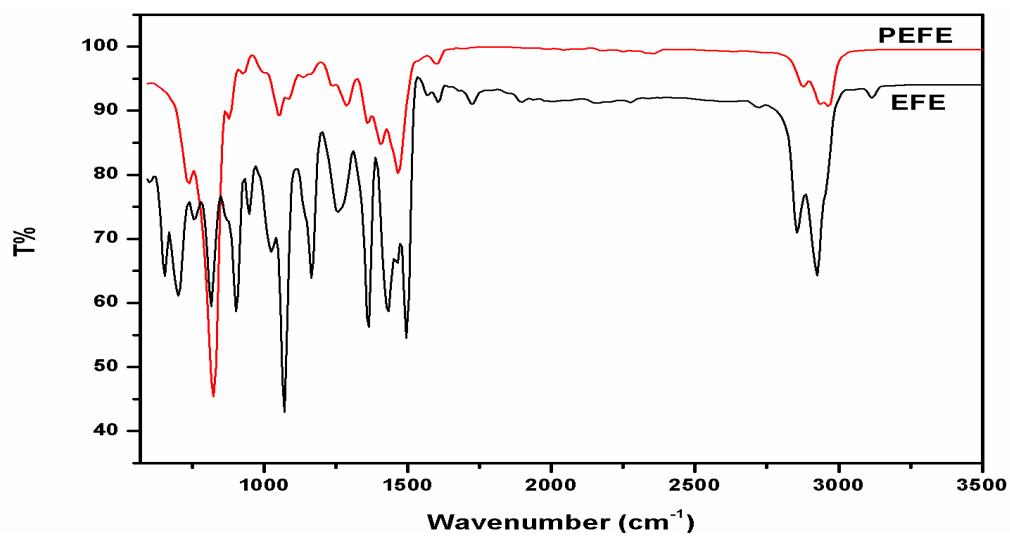


Figure B.2. FTIR spectrum for monomer **EFE** and its polymer **PEFE**